Fluoroprobe-Tagged Polysaccharide Vesicles for Drug Delivery Application

MS THESIS

SUBMITTED BY

RASIKA DAWARE

20141126

UNDER THE SUPERVISION OF

Prof. M. JAYAKANNAN

CHAIR

DEPARTMENT OF CHEMISTRY

INDIAN INSTITUTE OF SCIENCE EDUCATION AND RESEARCH PUNE

CERTIFICATE

This is to certify that this dissertation titled as "**Fluoroprobe- Tagged Polysaccharide Vesicles for Drug Delivery Application**" towards the partial fulfilment of the BS-MS dual degree programme at the Indian Institute of Science Education and Research, Pune represents study carried out by "**Rasika Virendra Daware** at IISER, PUNE" under the supervision of "**Prof. M. Jayakannan**, Professor, Chair, Department of Chemistry" during the academic year 2018-2019.

Rasika

Date: 20/03/2019

Place: IISER, Pune.

(Rasika Daware)

20141126

M.J

Date: 20/3/2019.

Place:

(Prof. M. Jayakannan)

DECLARATION

I hereby declare that the matter embodied in the report entitled "**Fluoroprobe- Tagged Polysaccharide Vesicles for Drug Delivery Application**" are the results of the work carried out by me at the Department of Chemistry, IISER PUNE, under the supervision of **Prof. M. Jayakannan** and the same has not been submitted elsewhere for any other degree.

Date: 20/03/2019

Place: IISER, Pune

(Raika Dawane)

20141126

Date: 20/3/2019.

Place:

(Prof. M. Jayakannan)

ACKNOWLEDGEMENT

I would like to take this opportunity to acknowledge my 5th year MS Thesis supervisor **Prof. M. Jayakannan** for his constant support and guidance throughout my project work. His encouragement and support has played a major role in the success of this journey. I would also like to thank him for providing the excellent lab facilities and exposure in learning.

I would also extend my gratitude to my Thesis Advisory Committee (TAC) member, Dr. Pinaki Talukdar, for being my TAC member and for his valuable remarks and suggestions during the TAC meetings.

Sincere thanks to Dr. Nilesh Deshpande, Dr. Sonashree and Mishika Virmani for all the help and aid that they have provided throughout this journey. A lot of things that I have learnt during this period are due to your constant help and guidance.

I am grateful to all the faculties in the Department of Chemistry, IISER Pune for their support and cooperation throughout my life at IISER.

I am indebted to all the technical staff at IISER Pune for their cooperation and service without which this journey wouldn't have been completed. I would like to thank Mahesh sir, Sandeep sir, Nitin sir, Ganesh sir and all other staff members for making my research easier and smooth at IISER Pune.

Without the support of my lab members Dr. Nilesh, Dr. Sonashree, Dr. Bhagyashree, Mehak, Mishika, Ruma, Dheeraj, Khuddus, Uttereshwar, Caroline, Sharada, Rahul, Akash and Pranav it would have been a difficult journey. Thank you all for helping me throughout my project and maintaining a friendly work environment.

I am thankful to all my friends who have always kept me going and motivated in all the hard times. Thank you for trusting me and keeping me up with a new spirit and enthusiasm.

Last but not the least, my family has been a constant support system. I would like to thank my mom, dad and sister Saniya for their emotional support and immense love and appreciation throughout all these years.

--- Rasika

CONTENT

LIST OF FIGURES AND TABLES

LIST OF ABBREVATIONS

AIE- Aggregation Induced Emission
PDP- 3- pentadecyl phenol
TPE- Tetraphenylethelene
Rh-B – Rhodamine –B
DLC-Drug Loading Content
DLE- Drug Loading Effeciency
DLS- Dynamic Light Scattering
FESEM- Field Emission Scanning Electron Microscopy

Abstract

Polysaccharide derived nano-carriers are emerging in drug/gene delivery area to cancer cells and are drawing a lot of attention. One of the major reason is the biocompatibility of these polysaccharides which is a very essential factor while designing a carrier for such biomedical applications. Design and synthesis of a fluorescent dextran nano-carrier for the delivery of the Cisplatin drug to the cancer cells has been shown in this report. The fluorescent tag on the polymer scaffold enables the tracking of the Cisplatin drug, which is otherwise difficult, given the non-fluorescent nature of the drug. Thus the system provides an insight in the fate of the polymer as well as the drug, giving us a twofold information. The fluorophore used in the system shows an Aggregation Induced Emission (AIE). Moreover, it makes an excellent FRET pair with Rhodamine – B dye. Knowing this, a fluorescent polymer with a tetraphenylethylene (TPE) chromophore substitution was made by first synthesising an acid derivative of the TPE molecule along with a substitution of a pentadecylphenol (PDP) unit to maintain the amphiphilicity of the polymer. An acid handle was incorporated to enable chemical conjugation of the Cisplatin drug. Further, this polymer was charecterized by ^{1}H and ^{13}C NMR spectroscopy and IR spectroscopy. Drug conjugation and dye loading studies were done. The size of the nanoparticle was charecterised using Dynamic Light Scattering (DLS). An enzyme degradation study was done to check the release kinetics and biodegradability. Further, an MTT assay was done to check the cytotoxicity of the polymers and cell killing in the cisplatin stitched counterpart

1. Introduction

Over the years, cancer has been one of the leading causes for an elevation in mortality rate[1,2]. Inspite of a lot of ongoing research in the delivery of drugs to cancer cells, only a few of the many developed systems reach the stage of clinical trials. Thus, more insight and better understanding is required to design a delivery system for the anticancer therapeutics. A lot of factors are involved in the successful delivery of the therapeutics to the desired site[3]. There are five major steps a nanocarriers has to go through, before it reaches the site of action. They are 1) Circulation in the blood 2) Accumulation at the site of the tumour 3) penetration through the tumour mass 4) internalisation of the nanocarrier by the cancer cells and 5) release of the loaded cargo[4]. This is known as CAPIR and this has to undergo a successful completion by the nanocarrier for achieving a maximum efficacy[4].

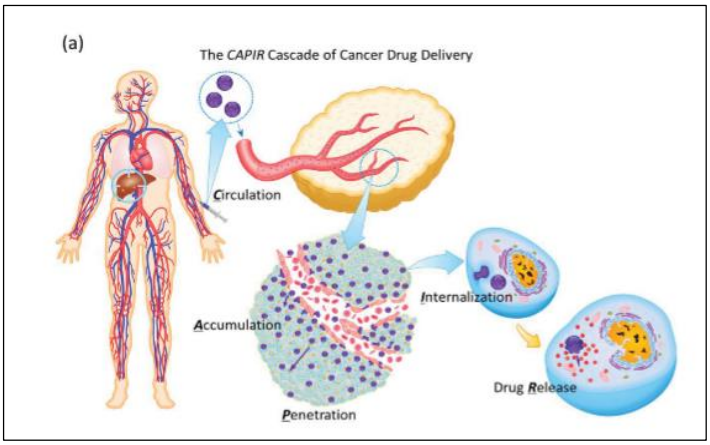

Figure 1.1 *CAPIR cascade for nanoparticle internalization*[5].

Free drugs can diffuse throughout the system and are non-target specific as a result of which, there are various side effects upon administration of the drugs in their native state[5]. Due to lack of differentiation between the healthy and the tumour tissue, a lot of damage is caused to the healthy cells as well[5]. Also, once into the system, the biodistribution, bioavailability, circulation period, and clearance are added factors which pose further challenges in the field of drug delivery[3,6]. Hence, developing a system which shows target specificity towards cancer cells, without affecting the healthy ones, and can overcome the above mentioned challenges is the need of the hour.

1.1 Why Nanocarriers?

Encapsulating the drug molecule in a nanocarrier can give many added advantages as compared to the free drug administration. Drug encapsulation can increase the solubility and hence the bioavailability of the drug. It can also help in improving the retention time of the drug in the system[6]. Moreover, nanocarriers can be engineered

in various ways to increase their target specificity and uptake. Attaching a target specific ligand on to the nanocarrier surface can enhance its uptake[7]. They can be structurally engineered to study the role of morphology (shape and size) of the carrier for drug delivery purpose[8].

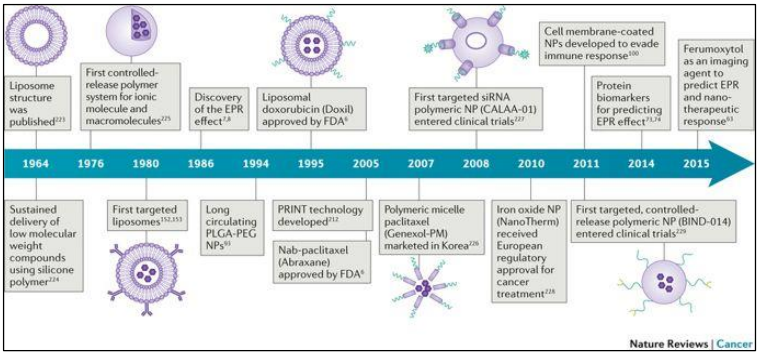

Figure 1.2 *Evolution of nanocarriers in cancer drug delivery*[13].

One such example is Doxil, a clinically used drug, which is essentially a liposomal formulation encapsulating the anticancer drug Doxorubicin[9]. Over the years many nano-assemblies such as synthetic polymers[10,11], dendrimers, carbon nanotubes, liposomes[12], gold nanoparticles, micelles, etc.[5]. have been studied to deliver the drugs. Farokhzad et al. in their review have shown the evolution and progress of nanocarriers in the drug delivery to cancer tissue[13].

1.2 The EPR effect

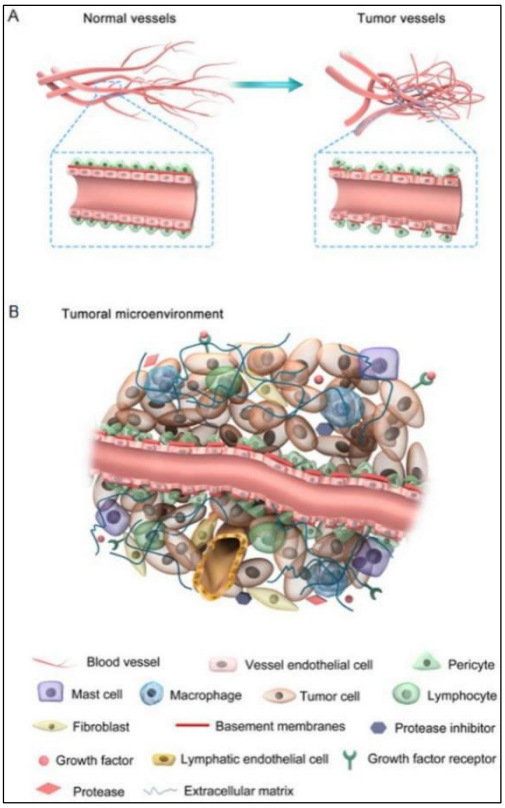

Figure1.3 *EPR effect*[14].

Normal cells are marked by characteristic features like tightly packed junctions and show the property of contact inhibition. Cancer cells on the other hand, lose this property of contact inhibition as a result of which there is rapid growth and differentiation of cells generating the tumour mass. This leads to disorientation in the alignment of the cells[14]. As a result, solid tumours are marked by unique characteristics like leaky vasculature and defective lymphatic drainage due to which nanocarriers get preferentially accumulated at the tumour site. This effect is known as the enhanced permeability and retention effect (EPR effect) [15] and is a passive way of targeting cancer cells.

Due to their large sizes (50 nm – 10 μm)[18], nanocarriers cannot penetrate through the tightly packed junctions of the endothelial cells of the healthy tissue. However, the endothelial cells are poorly packed in case of tumour tissues and there are large fenestrations associated with the cancer cells due to which nanocarriers can penetrate and preferentially accumulate in the solid tumours. Due to this preferential accumulation and retention at the tumour tissue, nanocarriers can chaperone the encapsulated therapeutics and increase its accumulation at tumour site, hence, increasing its therapeutic efficiency and local concentration at tumour tissue as compared to the free drug [18]. Moreover, tagging the nanocarrier with a targeting moiety can enhance the specificity and uptake by the cells. Such targeting is called as active targeting. A combination of both, active and passive targeting is a promising approach that is widely being explored since a combination of passive accumulation due to the EPR effect and the enhanced uptake due to the targeting moiety can maximise the therapeutic efficacy of an anticancer drug[16,17].

1.3 Biodegradable Polymers as Nanocarriers

With the advancements in designing of nanocarriers as potential candidates for achieving a target specific drug/gene delivery to cancer cells[6], biodegradability and biocompatibility of the materials used can become a major concern. Thus, more efforts have been put in designing and synthesising nanocarriers which are biocompatible as well as biodegradable. Having said that, polysaccharides are one class of biopolymers which are being extensively studied due to their biocompatibility[19,20]. The multiple functional groups on various polysaccharides can be synthetically modified and thus opens up a wide possibility of structural modifications. One such polysaccharide is dextran. It has a glucose repeating unit with mainly α – 1,6 glycoside linkages and the multiple hydroxyl functional groups present on it makes it highly hydrophilic in nature. Modifications can be made on the Dextran backbone with the help of these hydroxyl functional groups, thus, making it a suitable candidate for drug delivery applications. Also, Dextran is known to find its use as a plasma volume expander and anticoagulant[26]. Further, polysaccharides show like- like interactions with the lectins present on the surface of the cells, thus, leading to a better uptake of these nanocarriers by the cancer cells[21].

1.4 Fluorescent Polymers: Theranostics Applications

Tracking a nanocarrier inside the system gives a further insight into the fate of the nanocarrier, the route of intake, and the delivery of the drug to the cells. Hence, a major limitation of a non-fluorescent nanocarrier is the difficulty in tracking the cargo once it's inside the cell. Hence, these nanocarriers are usually loaded with a fluorescent drug/dye molecule to enable the tracing of the nanocarrier. A fluorescent tag on the nanocarrier can help in giving an insight into the fate of the nanocarrier, once it's into the system[22]. Further, it can give an added advantage in studying the uptake of non-fluorescent drugs like cisplatin, thus, giving a deeper insight and understanding of the drug delivery by the designed nanocarrier. It can, thus, ensure easy tracking and can be used for theranostic purpose.

1.5 Aggregation Induced Emission

In 2001, a very interesting phenomenon of Aggregation Induced Emission (AIE) was discovered by Hong et al. These chromophores, unlike conventional, are non-luminescent when dissolved in a solvent system. However, upon being in an aggregated state they show strong fluorescence. The restriction of the intramolecular rotation upon aggregation of the fluorophore is found to be the major reason for this unique phenomenon. One such chromophore is tetraphenylethelene (TPE)[23]. It can be used as a fluorescent tag to obtain AIE based fluorescent polymers. Polymer self-assembly can potentially induce aggregation of these chromophores while the disruption of the self-assembly would lead to the dissociation of the aggregated state, thus quenching the fluorescence. This can thus not only be used for monitoring the nanocarriers but would also give an added information of the disruption of the self-assembly. Thus, building such a system gives a 2 fold information in the fate of the nanocarrier.

1.6 Dextran Vesicles for Cancer Therapy

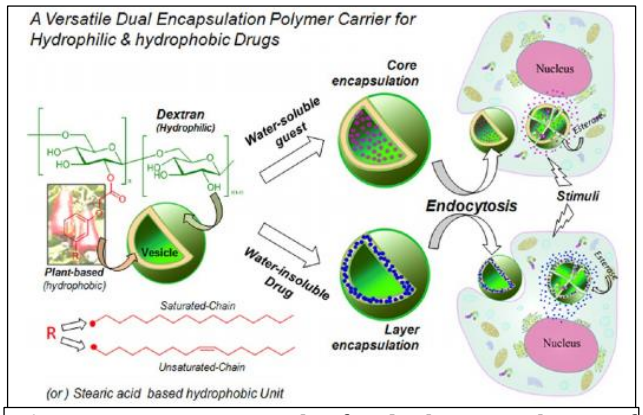

Figure1.4 *Dextran vesicles for dual encapsulation of hydrophilic and hydrophobic drug*[24].

Pramod et al. [24] have previously shown that modification of the dextran (mol. Wt. 6000) biopolymer with a 3-Pentadecyl phenol (PDP) unit (obtained from the liquid of cashew nut) led to the formation of dextran vesicles which can be used in the delivery of both, hydrophobic (water insoluble) as well as hydrophilic (water soluble) drugs. In this study, Dextran was modified with various hydrophobic units to obtain a vesicular morphology. However, only the substitution of PDP on to the dextran backbone lead to the formation of vesicular assemblies showing a unique packing between the PDP hydrophobic units leading to the formation of the vesicles. The crystal structure showed interdigitization between the hydrophobic units to form the bilayer. It was also observed that a substitution of more than 10% of PDP unit caused solubility problems. Thus, a vesicular morphology was designed and optimised for the delivery of hydrophobic and hydrophilic drugs to the cancer cells.

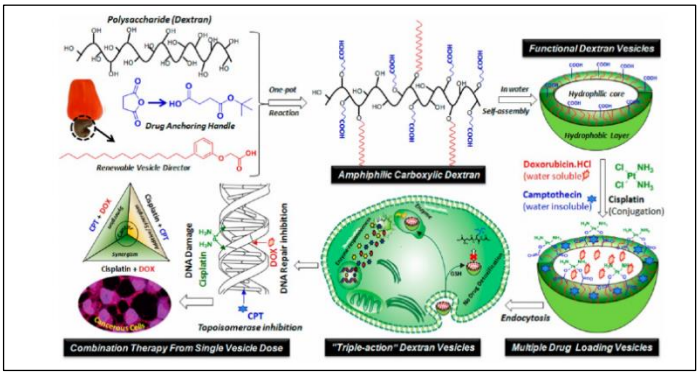

Figure1.5*: Cisplatin stitched vesicles for synergistic triple drug delivery to cancer cells*[25].

Further, Deshpande et al.[25] showed that, addition of a functional handle on the dextran hydrophilic backbone along with the PDP (hydrophobic) unit can enable chemical conjugation of therapeutic drug to the dextran polymer. Cisplatin was chemically stitched onto the dextran backbone to obtain a Cisplatin stitched polymer. Moreover, due to the vesicular morphology, these nanocarriers could be loaded with both, hydrophilic as well as hydrophobic drugs. Thus, combination therapy of Doxorubicin, Camptothecin and Cisplatin was achieved with a single nanocarrier platform to obtain synergistic killing in breast cancer cells[25].

However, these vesicles are non-fluorescent in nature and thus, information on the fate of the nanocarrier after the disassembly of the cargo cannot be inferred from the physically loaded system. Further, drugs like cisplatin are non-fluorescent and thus not much information can be acquired about its delivery unless coupled with a fluorescent probe. Thus, this thesis is aimed at extrapolating the previously established cisplatin stitched dextran polymer model to acquire further insight into the fate of the polymer and the cisplatin drug, by tagging the polymer with a chromophore. For this purpose, the tetraphenylethelene (TPE) chromophore was thought to be a good candidate due to its unique property of aggregation induced emission (AIE). Further, TPE is also known to show Foster Resonance Energy Transfer (FRET) with a hydrophilic dye Rhodamine-B. This gives an added advantage as the FRET between the two chromophores turns off upon the disruption of the self-assembly due to the increase in the distance between the two chromophores, giving an information of the cleavage of the vesicles. Studies were made to understand the FRET between the two chromophores. An MTT assay was done to check the killing of the cells and these vesicles will be further used for bio imaging of MCF-7 breast cancer cells. Thus, AIE based dextran fluorescent vesicles were structurally designed for bio-imaging and delivery of Cisplatin to cancer cells.

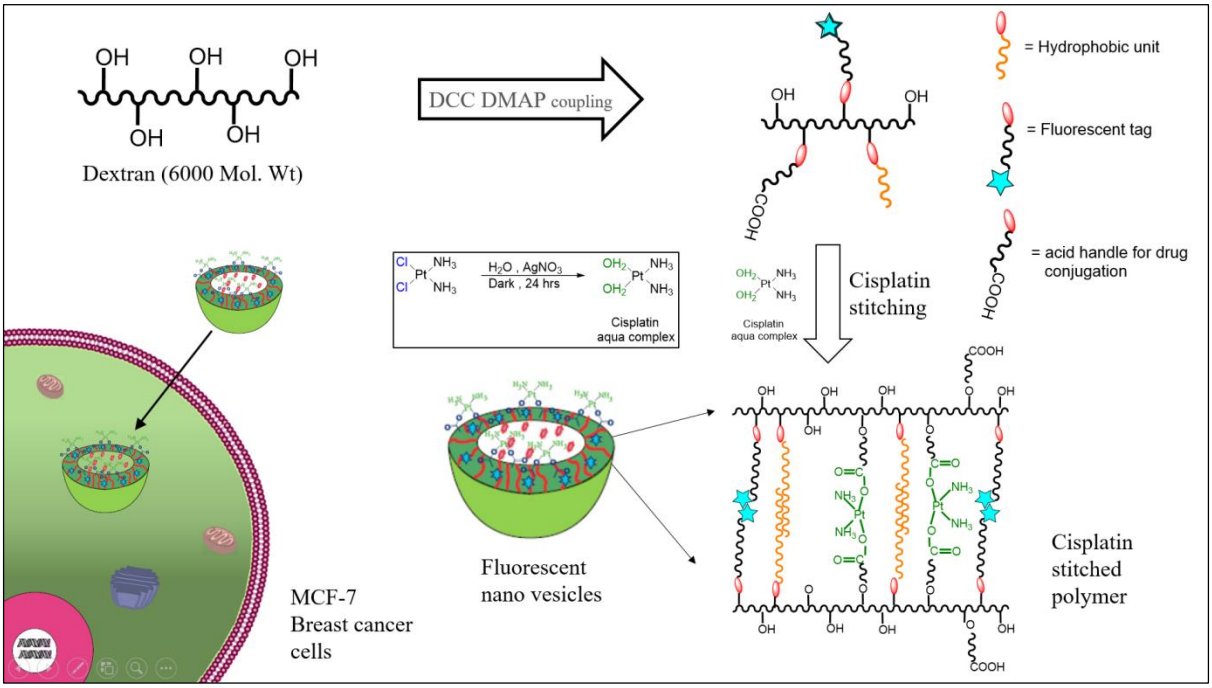

Figure1.6 *Schematic representation of the cisplatin stitched fluorescent vesicles for drug delivery to MCF-7 breast cancer cells.*

2. Experimental Section

2.1 Materials and Method:

3-Pentadecylphenol (PDP), Ethyl chloroacetate, Benzophenone, 4-hydroxy benzophenone, zinc powder, titanium tetrachloride, succinic anhydride,tertiary butanol, triethylamine (TEA) , N-hydroxy succinamide (NHS), Dextran (6000 MW), dicyclohexylcarbodimide (DCC), Cisplatin, Horse Liver Esterase enzyme, 4-dimethylamino pyridine (DMAP), Rhodamine-B, trifluoro acetic acid (TFA), were purchased from Aldrich Chemicals. Inorganic chemicals like NaOH, K_2CO_3 and all other essential reagents and organic solvents like dichloromethane (DCM), N,N dimethyl formamide (DMF), Dioxane, Tetrahydrofuran (THF) were purchased from a local vendor and purified by following the standardized protocol. Dimethylsulfoxide (DMSO) was dried using the standard protocol. Cryo stored MCF-7 breast cancer cells (passage (p) =22) were used for cellular studies. The cells were checked for mycoplasma contamination using DAPI. The cells were found to be in a good condition and were contamination free. The cells were cultured in DMEM media along with a supplementation of 5% fetal bovine serum (FBS). Detachment of cells was done using Tripsin and 96 well plates were used to seed the cells for all conducted studies.

2.2General Procedures:

1H NMR spectrums were recorded using a 400 MHz Jeol and 100- MHz Bruker NMR spectrometer. For recording the spectra, $CDCl_3$ and DMSO d_6 were used as solvents. These solvents contained a small amount of TMS which was used as an internal standard. The electronic spectra were recorded using Perkin- Elmer Lambda 45 UV-visible, and a Fluorolog HORIBA JOBIN VYON fluorescence spectrophotometer. This spectrophotometer has a 150 W Xe lamp (excitation source at 25ºC (R.T)). The sizes of the nano structures after self-assembly were determined using the Dynaic Light Scattering (DLS) technique. Nano ZS-90 apparatus which utilizes a 633nm red laser (from Malvern instruments) was used for the same. Zeiss Ultra Plus scanning electron microscope was used to take the FESEM images. Samples were dropcasted on a silicon wafer and dried at room temperature before imaging.

2.3 Synthesis

2.3.1 Synthesis of ethyl 2-(3-pentadecylphenoxy)acetate

3-Pentadecylphenol (PDP) (5.0 g, 0.016mol) was completely dissolved using 50 mL of dry DMF as a solvent. To this, K_2CO_3 (6.8 g, 0.049mol) and KI (a pinch) were added followed by refluxing at 80ºC for 30 minutes. This system was cooled to room temperature and dropwise addition of ethyl chloro acetate (3.0 g, 0.018mol) was done using a dropping funnel. The reaction was further kept on reflux for 24 h. Once the reaction was completed, DMF was removed from the system by vacuum distillation and 100 mL cold water was added to it. Further, extraction of the product was achieved by using ethyl acetate as an organic solvent along with water. The organic layer was separated using a separating funnel and passed through anhydrous sodium sulphate. Ethyl acetate was evaporated and further purification of the product was done by passing over a silica column. 4% ethyl acetate in pet ether was used as a solvent system. Obtained Yield = 4.72 g.

^{1}H NMR- (400MHz, $CDCl_3$) δ ppm: 7.17 – 7.13 (m , 1H), 6.79 – 6.66 (m , 3H), 4.57 (s, 2H), 4.26 – 4.21 (q , 2H), 2.55 – 2.52 (t, 2H), 1.56 (m, 2H), 1.28 – 1.23 (m , 27 H), 0.87 – 0.83 (t , 3H).

^{13}C NMR -(400MHz, $CDCl_3$) δ ppm : 168.87, 162.33, 157.67, 144.59, 129.03, 121.74, 114.86, 111.26, 65.25, 61.10, 36.28, 35.78, 31.76, 29.20, 22.52, 13.95

IR Wavenumber cm^{-1} – 3738.63, 3393.81, 2922.70, 2854.15, 2312.09, 1756.94, 1658.27, 1598.05, 1450.79, 1381.99, 1280.10, 1200.73, 1160.21, 1088.32, 1029.76, 930.78, 862.20, 775.54, 695.49, 602.39, 532.47.

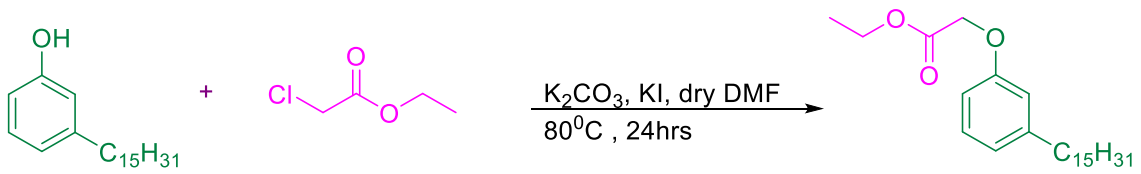

Scheme 2.1. Synthesis of PDP ester

2.3.2 Synthesis of 2-(3-pentadecylphenoxy)acetic acid

50 mL of Dioxane was taken in a round bottom flask and PDP ester (5.0 g, 0.012mol), was weighed and added to this solvent. Constant stirring (for 5 minutes) was done to ensure complete dissolution of PDP ester. To this, KOH (2.1 g, 0.038mol) was added and this system was refluxed at 100ºC for 24 h along with constant stirring. Dioxane was then concentrated under vacuum. To this, 200 mL Acid water (0.01 N HCl) was added and the product was extracted in ethyl acetate by using a separating funnel. The organic layer was passed through anhydrous Na_2SO_4 to ensure removal of trace amount of water. Further purification of the product was done by passing it through a silica gel column. A solvent system of 10% ethyl acetate in pet-ether was used to achieve the separation . Yield = 4.54 g

^{1}H NMR- (400MHz, $CDCl_3$) δ ppm: 7.23 – 7.02 (m , 1H), 6.86 – 6.72 (m , 3H), 4.68 (s, 2H), 2.61- 2.51 (t , 2H), 1.62 – 1.58 (m , 2H), 1.30 – 1.26 (m , 24 H), 0.91 – 0.87 (t, 3H).

^{13}C NMR -(400MHz, $CDCl_3$) δ ppm : 173.16, 157.27,145.08, 129.37, 122.39, 115.03, 111.36, 64.81, 35.95, 31.9329.70, 29.60, 29.51, 29.37, 22.70, 14.14.

IR Wavenumber cm^{-1} – 3882.35, 3737.51, 3364.90, 2916.28, 2845.31, 2582.20, 2180.36, 1724.48, 1653.37, 1463.71, 1420.60, 1274.17, 1159.55, 1100.23, 1018.72, 930.88, 765.67, 686.84.

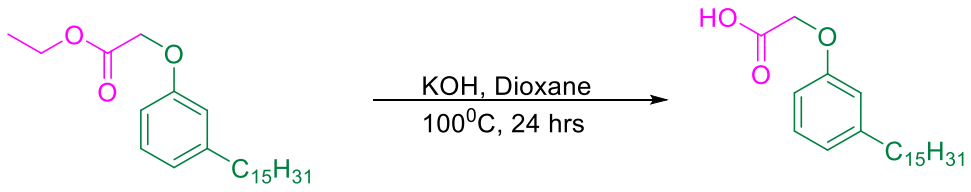

Scheme 2.2 Synthesis of PDP acid

2.3.3 Synthesis of 4-(1,2,2,-triphenylvinyl)phenol

Benzophenone (5.00 g, 27mmol) and 4-hydroxybenzophenone (5.44g, 28mmol) along with (4.46g, 69 mmol) Zinc powder were dissolved in dry THF and kept under N_2 conditions. The system was kept in an ice bath i.e. 0ºC

. (6.25g, 33mmol) $TiCl_4$ was slowly added to the reaction in a drop-wise manner and the mixture was kept at stirring for 30 minutes. The reaction was refluxed at 70ºC for 12 h. After 12 h, the system was cooled to room temperature and THF was concentrated at reduced pressure. About 50 mL 1 N HCL solution was added and ethyl acetate was used as an organic solvent to extract the product. After separation of the organic layer using a separation funnel, the organic layer was passed through anhydrous sodium sulphate and the solvent evaporated to obtain the crude. Further, a silica gel column with 2% ethyl acetate pet-ether as a solvent system was used to separate the desired product from the crude. Yield = 2.94 g.

^{1}H NMR- (400MHz, $CDCl_3$) δ ppm: 7.15 - 7.01 (m , 15 H) , 6.91 – 6.89 (m , 2H), 6.59 – 6.56 (m , 2H), 4.66 (s, 1H).

^{13}C NMR - (400MHz, $CDCl_3$) δ ppm : 153.98, 143.98, 143.87, 140.41, 140.18, 136.37, 132.73, 131.32, 127.60, 126.26, 114.57, 77.33, 77.02, 76.70.

IR Wavenumber cm^{-1} – 3321.12, 2128.34, 1639.20, 1257.91, 1021.18, 691.73, 546.0.

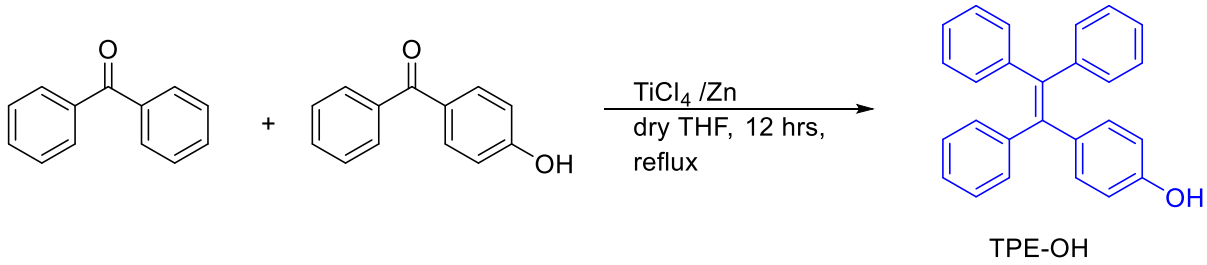

Scheme 2.3 Synthesis of TPE - OH

2.3.4 Synthesis of ethyl 2-(4-(1,2,2-triphenylvinyl)phenoxy)acetate

In a two neck round bottom flask, TPE-OH (4.00g, 11.4mmol) and K_2CO_3 (2.38g, 17.2mmol) were weighed and dissolved by adding 65 mL Acetonitrile as a solvent. The system was kept at stirring for 30 minutes at 80ºC. (1.92g, 11.4mmol) ethyl chloroacetate was added slowly in a drop-wise manner to the system after letting the system to come back to the room temperature. After addition, the system was heated at 90ºC for 12 h with stirring. Cooling down of the system to room temperature followed by filtration for removal of K_2CO_3 was done. Concentration of acetonitrile was achieved under reduced pressure. About 100 mL water was added to this and the desired organic product was extracted using ethyl acetate. The organic layer was separated

using a separating funnel and was passed through anhydrous sodium sulphate. The product was further purified by running a silica gel column with 5 % ethyl acetate in pet ether as an eluent. Yield = 3.60 g

^{1}H NMR- (400MHz, $CDCl_3$) δ ppm : 7.12 – 7.02 (m, 15H),6.96 - 6.94 (m , 2H), 6.66 – 6.64 (m , 2H), 4.55 (s, 2H), 4.27 (q, 2H), 1.29 (t , 3H).

^{13}C NMR -(400MHz, $CDCl_3$) δ ppm : 168.89, 156.30, 143.86, 143.82, 140.41, 140.24, 137.16, 132.56, 131.30,127.71, 127.60, 126.29, 113.79, 77.33, 77.02, 76.71, 65.35, 61.31, 14.15.

IR Wavenumber cm^{-1} – 3407.80, 3054.51, 2982.87, 2926.41, 2312.48, 1955.70, 1885.54, 1814.95, 1750.16, 1657.16, 1601.46, 1500.63, 1441.72, 1380.99, 1286.74, 1188.68, 1077.59, 1023.15, 917.49, 825.53, 752.06, 695.25, 607.87.

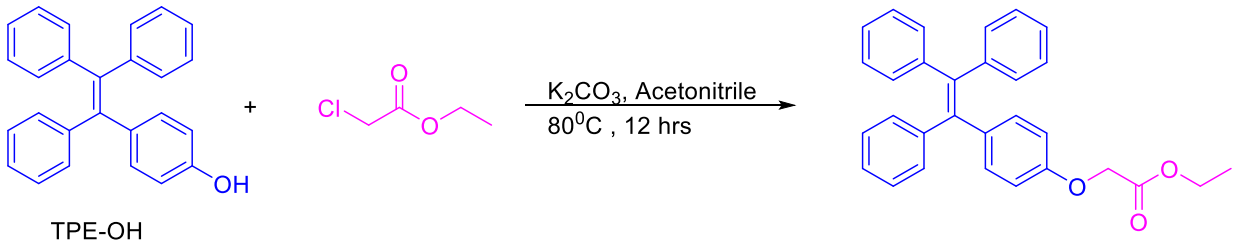

Scheme 2.4 Synthesis of TPE ester

2.3.5 Synthesis of 2-(4-(1,2,2-triphenylvinyl)phenoxy)acetic acid

TPE ester (3.50g, 8.06 mmol) and KOH (1.35g, 24.19 mmol) were weighed and dissolved in 40 mL dioxane (by stirring for 5 minutes). For the next 6 h, the reaction mixture was kept for reflux at 100ºC. System was then brought down to room temperature and the organic solvent (Dioxane) was removed from the system under reduced pressure. A solid compound was obtained after concentration of the solvent. This was further dissolved in acidic water (pH 6) and the product was extracted using an organic solvent, ethyl acetate. A separating funnel was used to separate the two layers and the organic layer was dried over anhydrous sodium sulphate. The desired product was further purified and separated by running a silica gel column in which 10% ethyl acetate in pet ether was used as a solvent system. Obtained Yield = 3.00 g

^{1}H NMR- (400MHz, $CDCl_3$) δ ppm: 7.02 – 6.96 (m , 15H), 6.79 – 6.77 (m , 2H), 6.46 – 6.44 (m , 2H), 3.72 (s, 2H).

^{13}C NMR -(400MHz, $CDCl_3$) δ ppm: 171.25, 155.89, 143.80, 143.72, 140.35, 140.19, 137.12, 132.57, 131.29, 128.49, 127.75, 127.64, 127,59, 126.36,113.99, 77.33, 77.01,76.70 , 67.06, 60.44, 21.06, 14.20

IR Wavenumber cm^{-1} – 3884.26, 3739.99, 3385.24, 2531.60, 2309.40, 2123.35, 1602.01, 1503.52, 1434.09, 1333.96, 1283.55, 1227.79, 1179.26, 1070.75, 824.80, 753.35, 698.31, 619.01.

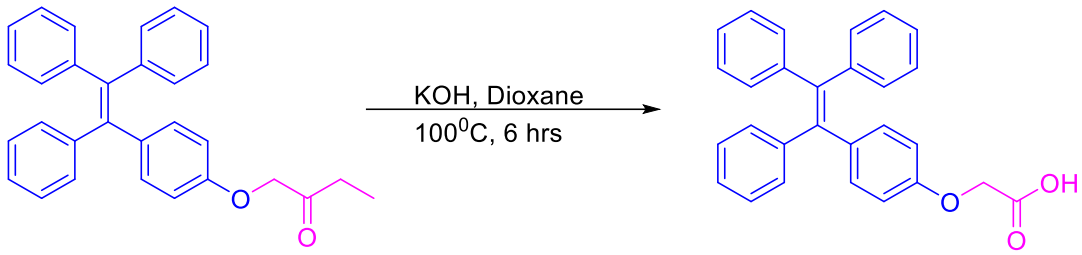

Scheme 2.5 Synthesis of TPE acid

2.3.6 Synthesis of tert- butyl ester of Succinic acid

Succinic anhydride (5.00g, 50mmol) , triethylamine (2mL , 15 mmol) , N- hydroxyl succinimide (1.72 g, 15 mmol), Dimethyl aminopyridine (0.62 g, 6mmol) were weighed in a round bottom flask and dissolved by adding 50 mL dry tolouene. *tert*- butyl alcohol was then added (using a syringe) to the reaction mixture and the system was kept at reflux at 110ºC for 24 h. The solution was allowed to cool down to the 25ºC (room temperature). To this, 50 mL ethyl acetate was added followed by multiple washings with 10% citric acid and brine solution. The organic layer was separated using a separating funnel and passed over anhydrous Na_2SO_4 to ensure the removal of traces of water. A yellow –brown liquid crude product was obtained after concentration the organic layer. The crude was further passed over a silica column in which a 10 % ethyl acetate in pet ether solvent system was used to obtain a pure product. Yield = 3.12g

^{1}H NMR- (400MHz, $CDCl_3$) δ ppm : 2.61- 2.59 (t , 2H), 2.54 – 2.52 (t, 2H), 1.43 (s, 9H).

^{13}C NMR -(400MHz, $CDCl_3$) δ ppm : 178.25, 171.38, 81.02, 30.10, 29.14, 28.02.

IR Wavenumber cm^{-1} – 2979.11, 2932.25, 1712.29, 1366.70, 1243.48, 1146.11, 1034.45, 952.89, 896.79, 842.77, 756.20, 568.30

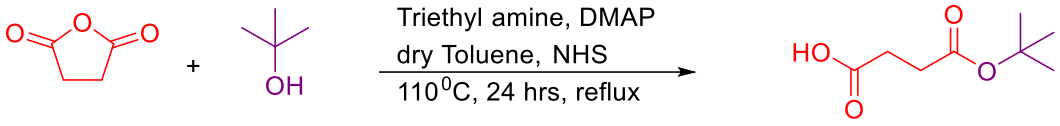

Scheme 2.6 Synthesis of *tert*- butyl ester of succinic acid

2.3.7 Synthesis of DEX-PDP-TPE-SA

Dextran (2.00 g, 12.20 mmol) , tert – butyl succinate (1.08 g , 6.20 mmol) , PDP acid (1.12 g, 2.10 mmol) , TPE acid (0.30g, 0.74 mmol) were dissolved using dry DMSO (50 mL) and were kept for N_2 purging for 30 minutes. To this reaction mixture, DCC (2.66 g, 12.9 mmol) and DMAP (0.38 g , 2.10 mmol) dissolved in dry DMSO were added. The reaction was continued to stir at 25ºC (room temperature) for next 24 h. DCU was formed as a byproduct of the reaction which settled as a white precipitate. This DCU precipitate was removed by filtration using Whatmann filter paper. This was followed by concentration of DMSO using vacuum distillation. The polymer was then precipitated using cold methanol as a bad solvent. The solid was filtered and multiple washes of methanol were given to ensure removal of any residual impurities. The product was then dried in vaccum oven at 60ºC to obtain a solid yellowish white product. Yield 1 g

^{1}H NMR- (400MHz, DMSO – d_6) δ ppm : 7.16 – 6.71 (m , 23H, Ar – H), 4. 63 (s, dextran anomeric proton) 4.47, 4.82, 4.88 (s , hydroxyl of dextran), 3.12 – 3.70 (dextran glucosidic protons), 1.48 (2 H, Ar-CH_2-CH_2) 1.34 (s, 9H, *tert*-butyl), 1.18 – 0.80 (aliphatic protons).

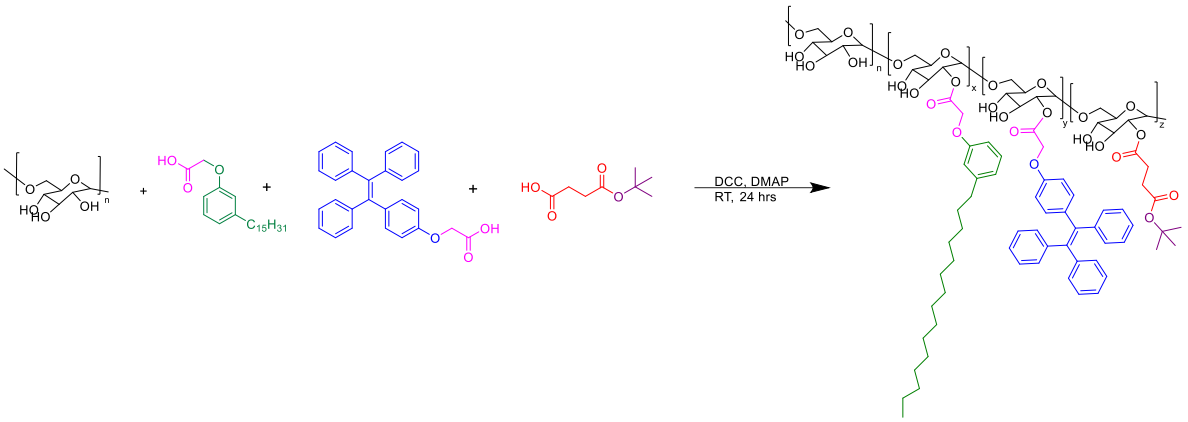

Scheme 2.7 Synthesis of DEX-PDP-TPE-SA

2.3.8 Deprotection of DEX-PDP-TPE-SA

The above synthesised polymer was further subjected to TFA deprotection to obtain the acid functionalized polymer. For the same, (0.25 g, 0.75 mmol) dextran derivative was dissolved in 5 mL DMSO in a 25 mL round bottom flask. To this, (1.2 mL, 15 mmol) TFA was added dropwise while continuous constant stirring at room temperature. The reaction was continued to stir for 4 h. Reduced pressure conditions were used to remove TFA and precipitation of polymer in methanol was done. The polymer was separated by filtration. It was further purified by dialysis against mili - Q water for 24 h followed by lyophilizing the sample. This sample was then used for further experiments.

^{1}H NMR- (400MHz, DMSO – d_6) δ ppm : 7.16 – 6.71 (m , 23H, Ar – H), 4. 63 (s, dextran anomeric proton) 4.47, 4.82, 4.88 (s , hydroxyl of dextran), 3.12 – 3.70 (dextran glucosidic protons), 1.48 (2 H, Ar-CH_2-CH_2), 1.18 – 0.80 (aliphatic protons).

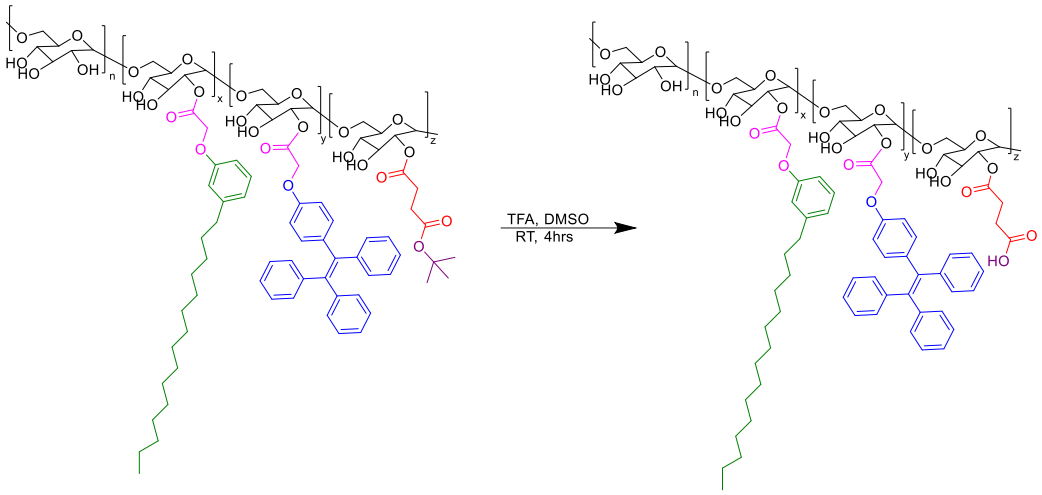

Scheme 2.8 Deprotection of DEX-PDP-TPE-SA

2.3.9 Synthesis of Cisplatin aqua complex [$Pt(NH_3)_2(OH_2)_2$]$^{2+}$

The aquated cisplatin complex was synthesised following the protocol mentioned in our earlier reports[27]. Cisplatin drug (20 mg , 0.066 mmol) was weighed and completely dissolved in (20 mL) mili – Q water. To this, Silver nitrate (22.5 mg, 0.132 mmol) was added and the system was kept at stirring for 24 h at 37ºC in dark. A milky white precipitate of silver chloride is produced which confirms the formation of the aquated complex of cisplatin. This precipitate was them removed by centrifugation and filtration (0.4 µm filter was used for this purpose). Lyophilisation of the resulting solution gave a light green coloured powder. This was then stored at 4ºC for further use.

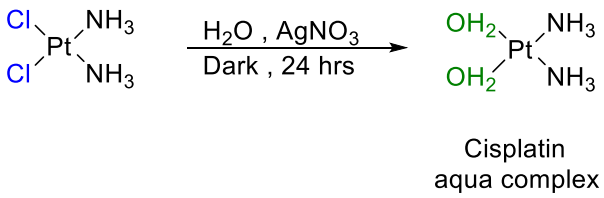

Scheme 2.9 Synthesis of Cisplatin aqua complex

2.3.10 DEX-PDP-TPE-SA polymer conjugation with cisplatin

To conjugate the cisplatin aqua complex with the synthesised dextran polymer, 20.00 mg of the polymer was weighed accurately and completely dissolved in 4 mL of mili Q

water by stirring and sonication. To this, 200 µL of NaOH solution (1 mg/ mL) was added and stirred for 30 minutes at 37^{o} C in dark. 3.4 mg (0.012 mmol) cisplatin aqua complex was added to this polymer containing solution and the system was kept at stirring for another 48 h at 37ºC , in dark. (MWCO = 3500) dialysis bag and mili – Q water was used for dialysis. The system was dialysed for next 24 h. The water in the reservoir was changed periodically to remove the unencapsulated and unwanted impurities. After 24 h, the solution from the dialysis bag was removed and filtered through a 0.4 µm filter. Lyophilisation of the sample was done to remove water and obtain a solid. It was then stored at 4ºC for further use. An OPD assay was done to calculate the drug/ dye loading content (DLC) and drug/ dye loading efficiency (DLE) of the polymer.

2.4. OPD assay for determining DLC and DLE

A stock solution (4mg /mL) was made by dissolving the lyophilised sample of the cisplatin stitched polymer in mili-Q water. OPD (*ortho*-phenylenediamine) solution of 1.2 mg / mL concentration was made by dissolving OPD into HPLC grade DMF and 80 µL of the stock solution was added to 2 ml of the OPD solution. The mixture was then heated at 80ºC for 2 h. in dark. The absorbance was recorded for the resulting solution at 706 nm and the molar extinction coefficient used was 24310 L mol^{-1} cm^{-1}. Calculation of DLC and DLE were done using the following equations[27]:

DLC (%) = {weight of drug in NP/ weight of drug loaded NP} x 100

DLE (%) = { weight of drug in NP/ weight of drug in feed} x 100

2.5 Dye encapsulation in dextran derivatives

10.0 mg of the dextran polymer was taken along with 1.0 mg of of Rhodamine-B dye and 1.0 mL of DMSO was used to dissolve the dye and polymer. This was kept at stirring for 15-20 mins To this solution then, dropwise addition of 1.0 mL of mili-Q water was done and the system was kept at stirring in dark for 12 h. After 12 h, it was transferred in to a dialysis bag (MWCO = 3500) and kept for dialysis against a large amout of mili-Q water for 48 h while periodically changing the water in the reservoir to ensure the removal of unencapsulted and unwanted molecules. After dialysis, the solution from the bag was filtered using a 0.45 µ whattman filter paper followed by lyophilisation and stored at 4^{oC} for further use. Beer – Lambert's law was used to determine the amount of dye encapsulated in the polymer sample. The molar extinction coefficient used for the calculations was 1,06,000 L cm^{-1} mol^{-1} . The DLC and DLE were calculated following the equations given below.

DLC (%) = {weight of dye in NP/ weight of dye loaded NP} x 100

DLE (%) = { weight of dye in NP/ weight of dye in feed} x 100

2.6 *In vitro* release kinetics for Cisplatin drug:

To study the release kinetics of the cisplatin conjugated polymer, a drug release study at physiological pH was carried out using dialysis method. 3.00 mg of cisplatin conjugated polymeric vesicles were weighed and transferred to a dialysis bag in 3.0 mL of mili- Q water. It was dialysed against 10 mL (Phosphate Buffer Saline) PBS 7.4 pH in the reservoir at 37ºC along with a constant stirring. In another such setup, 10 units of esterase was added to the dialysis bag and the system was dialysed against 7.4 pH PBS at 37^{oC} at constant stirring. 0.4 mL of aliquots were taken from the reservoir at specific time point and replaced with equal volumes of fresh PBS solution. The released amount was calculated by doing an OPD assay of the aliquots. The calculation of percentage cumulative release was done using the following equation[27];

Cumulative release (%) = { C_n x V_0 / m } x 100

Where, C_n = amount of loaded cisplatin in n^{th} sample

V_0 = total volume

m = total amount of cisplatin loaded in vesicles

2.7 *In vitro* release kinetics of Rhodamine-B dye

In vitro release of Rhodmine-B from the dextran polymer was studied by dialysis method. 3.0 mg of dextran vesicles were dissolved in 1.0 mL of mili- Q water. This was added to a dialysis bag (MWCO = 3500) and immersed in a beaker containing 10.0 mL Phosphate Buffer Saline (PBS) 7.4 pH solution as a reservoir and stirred constantly at 37ºC. Similar setup was made for the enzyme assisted release of Rhodamine-B where typically, 10 U of esterase enzyme was added to the dialysis bag along with the dextran vesicles. To determine the amount of drug released, 2.0 mL of dialysate was removed periodically and the absorbance was measured for the same.

Cumulative release (%) = { amount of dye released at time t / total amount of dye taken in dialysis tube } * 100

2.8 Cell viability assay

A cell viability assay was performed in MCF-7 breast cancer cell line. Tetrazolium salt, 3-4,5 dimethylthiazol-2,5- diphenyl tetrazolium bromide (MTT) was used to check and compare the cytotoxicity of the free drug and the drug loaded polymeric carriers. A 96 well plate was seeded with 100ºCells per well in 100 µL of complete DMEM. The cells were allowed to adhere for next 16 h. Different concentrations of the polymer carrier and free drug were added to the cells and the cells were further incubated for 72 h. After the incubation period, the media was aspirated followed by the addition of 100 µL of freashly prepared MTT solution of 5mg/mL concentration (in complete media). The cells were further kept for incubation for 4 H at 37ºC. Formazan crystals were formed which were then dissolved in 100 µL of DMSO and the absorbance measurements were done at 570 nm using a variosacan micro plate reader. The data represents a mean value of three independent measurements. A graph of relative percentage values, as compared to the control , was plotted against the change in concentration.

3. Results and Discussion

3.1 Synthesis and characterization of monomers

Chemical conjugation of the therapeutic drug to the polymer backbone holds an added advantage over physical loading of the drug into polymeric self-assemblies. This can be achieved by adding a functional handle on the polymeric backbone which can be used to anchor the drug moiety to the polymer scaffold. Since, a chemical linkage is used to anchor the drug to the polymer, leaching from the nano-assemblies is less as compared to the physically loaded cargos. In this report, Cisplatin, an anticancer drug was chemically conjugated to the dextran polymer backbone. This dextran polymer was also modified with a fluorescent tag which enables the monitoring of cisplatin drug delivery in the system which is difficult otherwise, given the non-fluorescent nature of the drug. A fluorescent Dextran polymer was synthesised following the procedure mentioned in the experimental section. The synthetic scheme for the synthesis of the monomers is shown in. (Fig. 3.1).

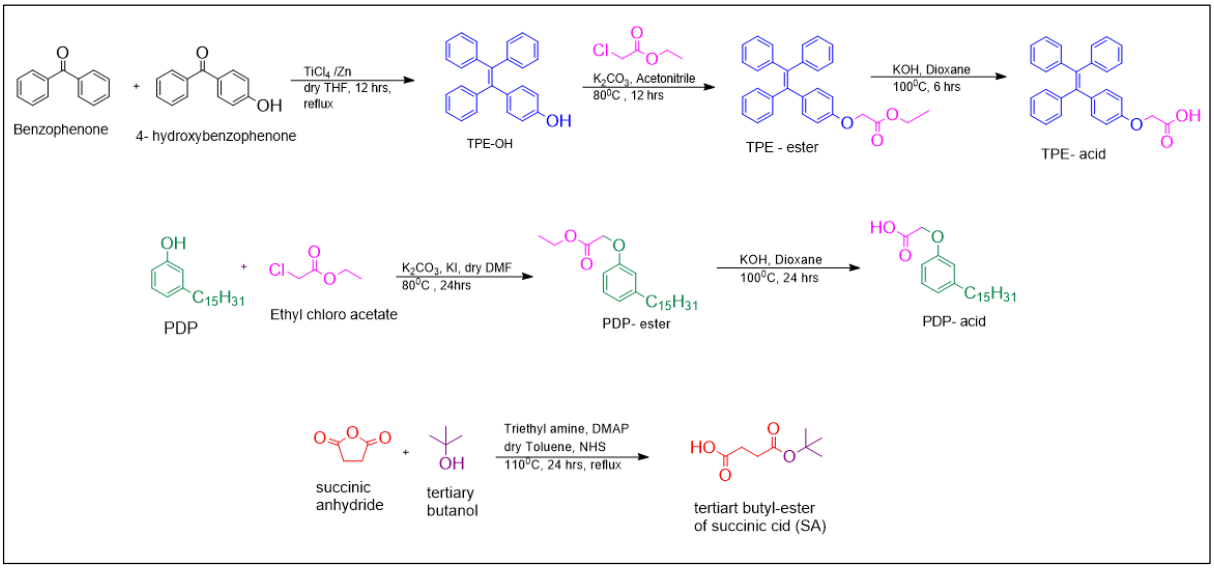

Figure 3.1 Synthetic scheme of the synthesis of the monomers .

Here, PDP (3- pentadecylphenol) was used as a hydrophobic unit of substitution to obtain the desired amphiphilicity for the self-assembly. From the previous established knowledge in our group, PDP is known to be a vesicle directing unit [24] and thus its incorporation as a hydrophobic unit should lead to the formation of a vesicular self-

assembly. Furthermore, it is extracted from the cashew nut shell and hence is biocompatible in nature. To obtain the desired hydrophobic unit, PDP was first coupled with Chloro ethyl acetate to obtain an ethyl ester of PDP which was further hydrolysed to obtain the PDP acid. Synthesis of this hydrophobic unit was confirmed by characterisation through ^{1}H and ^{13}C NMR spectrum.

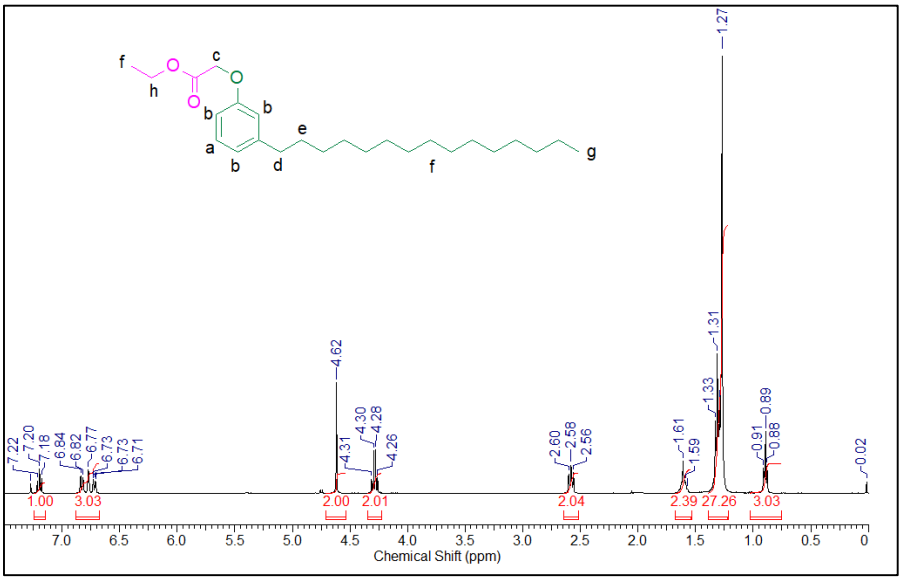

Figure 3.2. ^{1}H NMR of PDP ester

The formation of the PDP ester is confirmed by the ^{1}H NMR shown in fig (3.2) which shows a quartet at 4.28 ppm and a singlet at 4.62 ppm corresponding to the protons from the ethyl ester (fig 3.2).

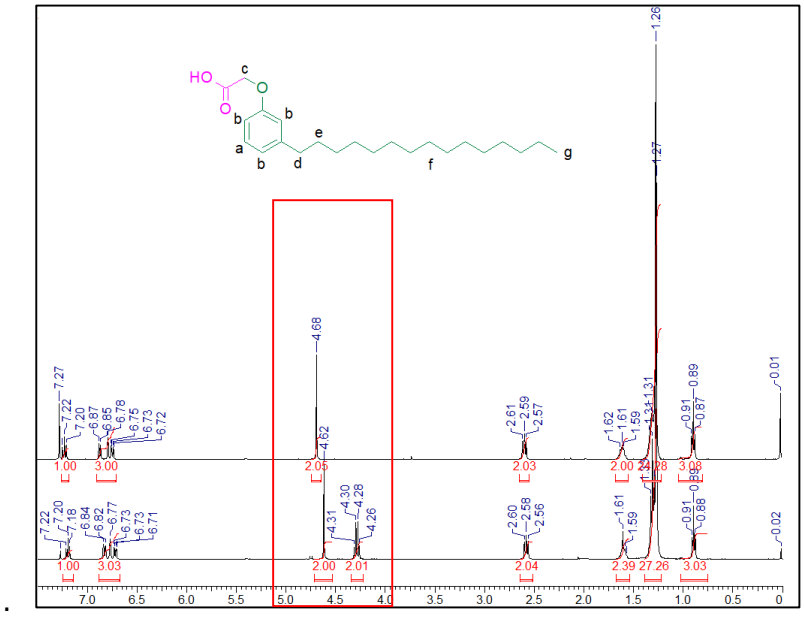

Figure 3.3.^{1}H NMR of PDP acid

On hydrolysis of the ester, the quartet at 4.28 ppm disappears and the singlet at 4.62 ppm shifts to 4.68 ppm due to the conversion of ester to acid functionality Fig (3.3).

Further, to obtain the fluorescent polymer, TPE fluorophore was conjugated to the dextran backbone. For the same, TPE- OH was first synthesised using McMurry coupling of benzophenone and 4- hydroxybenzophenone. This was then coupled with Chloro ethyl acetate to obtain a TPE ester which was then hydrolysed to obtain the TPE acid. The NMR in the figure (3.4) shows the formation of the TPE-OH.

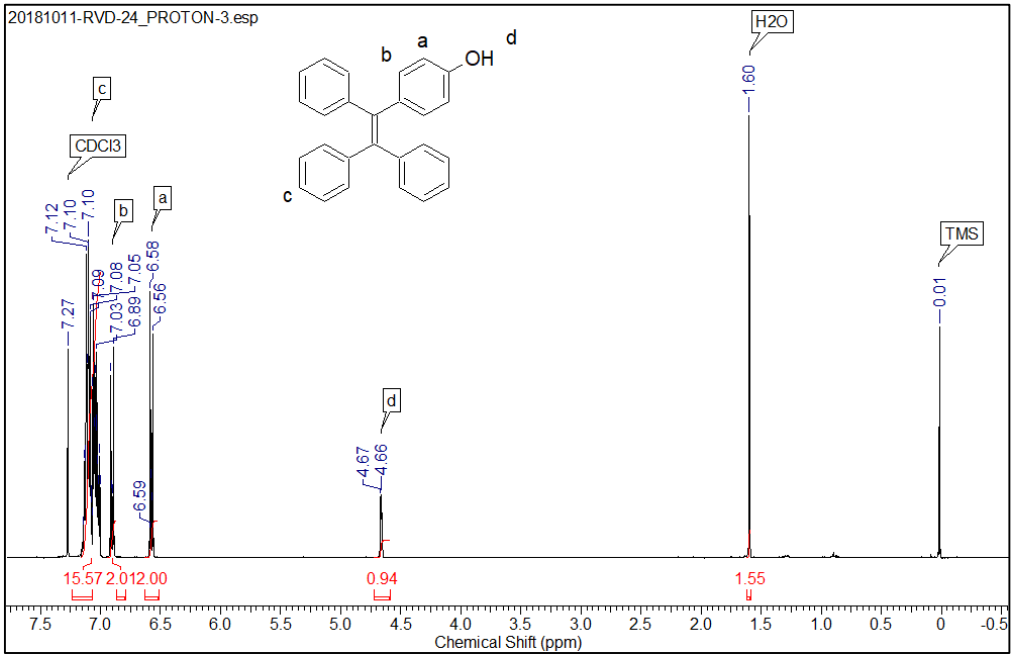

Figure 3.4. *^{1}H NMR of TPE-OH*

The multiplet at 7.12 ppm marks the 15 aromatic protons while the aromatic OH proton appears at 4.67 ppm as a singlet.

The TPE-OH was coupled with ethyl chloroacetate and the ^{1}H proton NMR spectrum is shown in the figure (3.5). The disappearance of the peak corresponding to the aromatic OH proton was observed corresponding to the formation of product. Also, three new peaks appear at 4.56 ppm (singlet), 4.26 ppm (quartet) and 1.29 ppm (triplet) as we can see in figure (3.5). Appearance of these peaks confirm the formation of the ethyl ester of TPE.

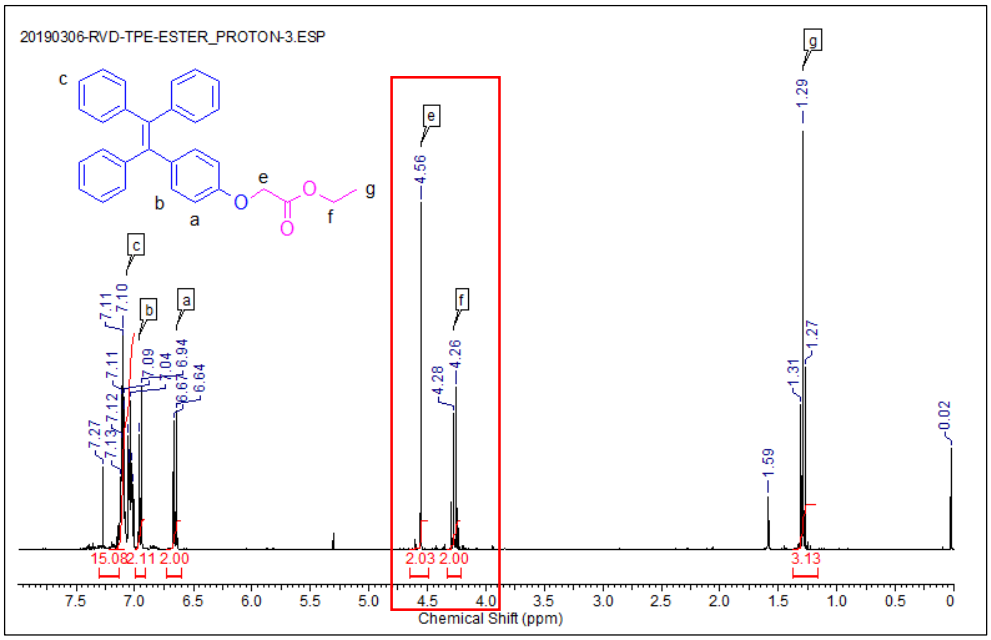

Figure 3.5. ^{1}H NMR of TPE- ester

Further, the ethyl ester was hydrolysed to obtain the TPE acid and same can be confirmed from fig (3.6). The quartet and the triplet at 4.26 ppm and 1.29 ppm respectively (in the ester NMR) in figure 3.5 were observed to disappear after hydrolysis.

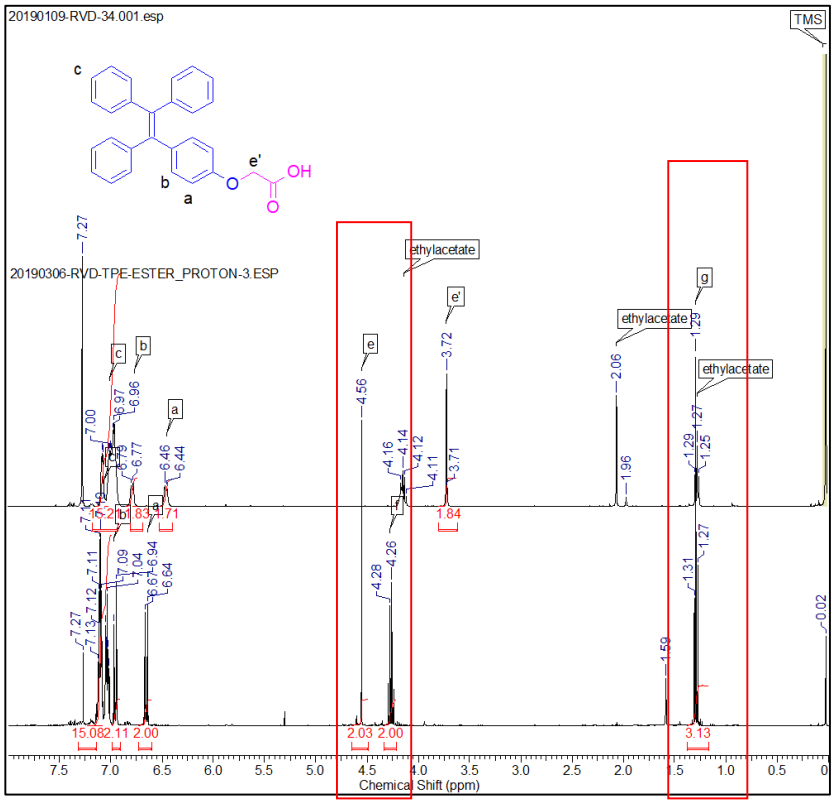

Figure 3.6. ^{1}H NMR of TPE- acid

Moreover, Succinic anhydride was ring opened using *tert*- butanol to obtain tertiary butyl ester of succinic acid. The formation of the tertiary butyl ester of succinic acid was confirmed by the peak at 1.43 ppm corresponding to the 9 protons in the tertiary butyl unit as shown in the figure (3.7). This was then used as functional handle for cisplatin conjugation on the polymer after deprotection.

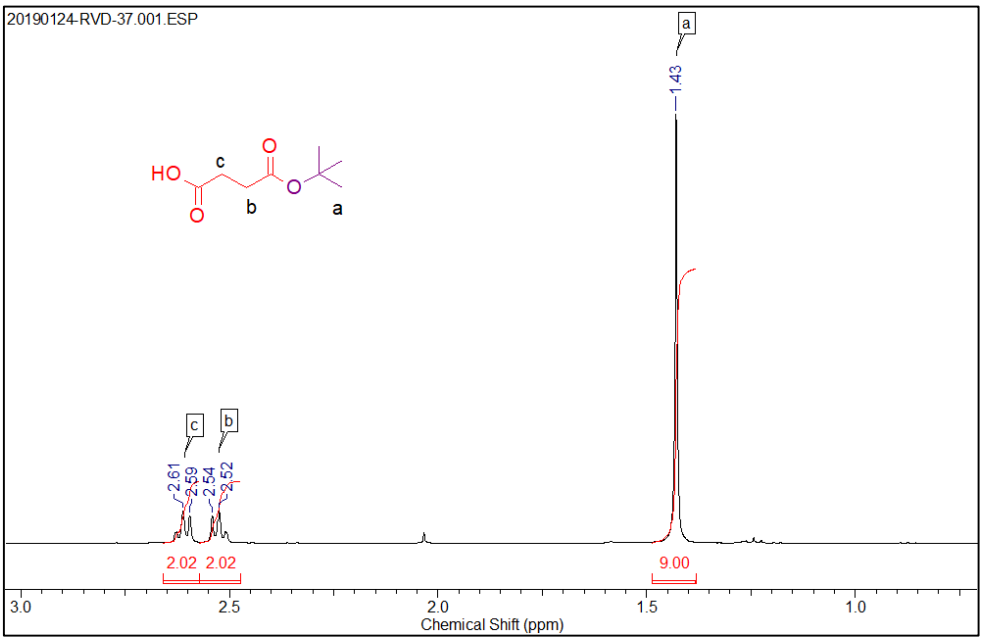

Figure 3.7. ^{1}H NMR of tertiary butyl ester of succinic acid

3.2 Synthesis of DEX-PDP-TPE-SA

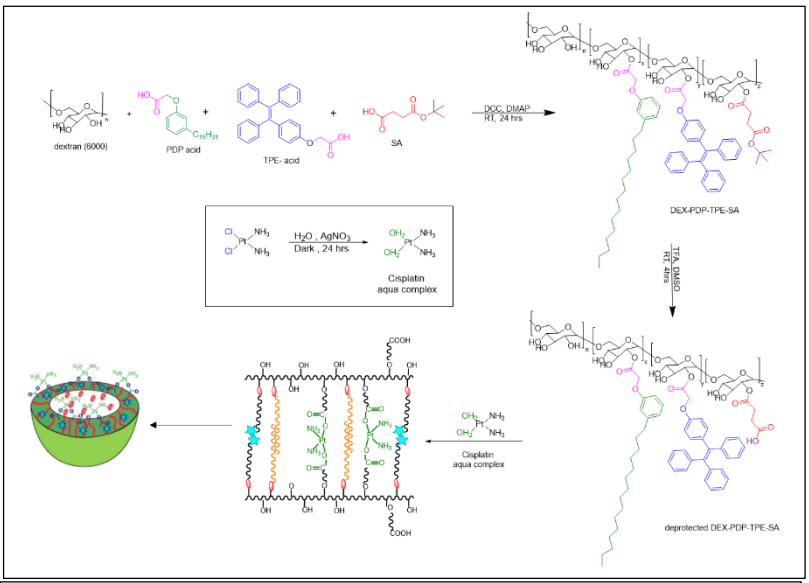

Figure 3.8 Synthetic scheme for the synthesis of the fluorescent cisplatin stitched vesicles.

The fluorescent polymer was synthesised by adding Dextran with PDP acid, TPE acid and tert-butyl ester of succinic acid using DCC/DMAP coupling in a one pot reaction. Fig. (3.8) shows a schematic representation of the synthesis and self-assembly of the polymer.

Coupling of these acids on the dextran backbone results in the formation of an ester linkage which can be cleaved by action of enzymes like esterase in the cellular compartments. 20.0 mg of DEX-PDP-TPE-SA polymer was subjected to self-assembly by the dialysis method.

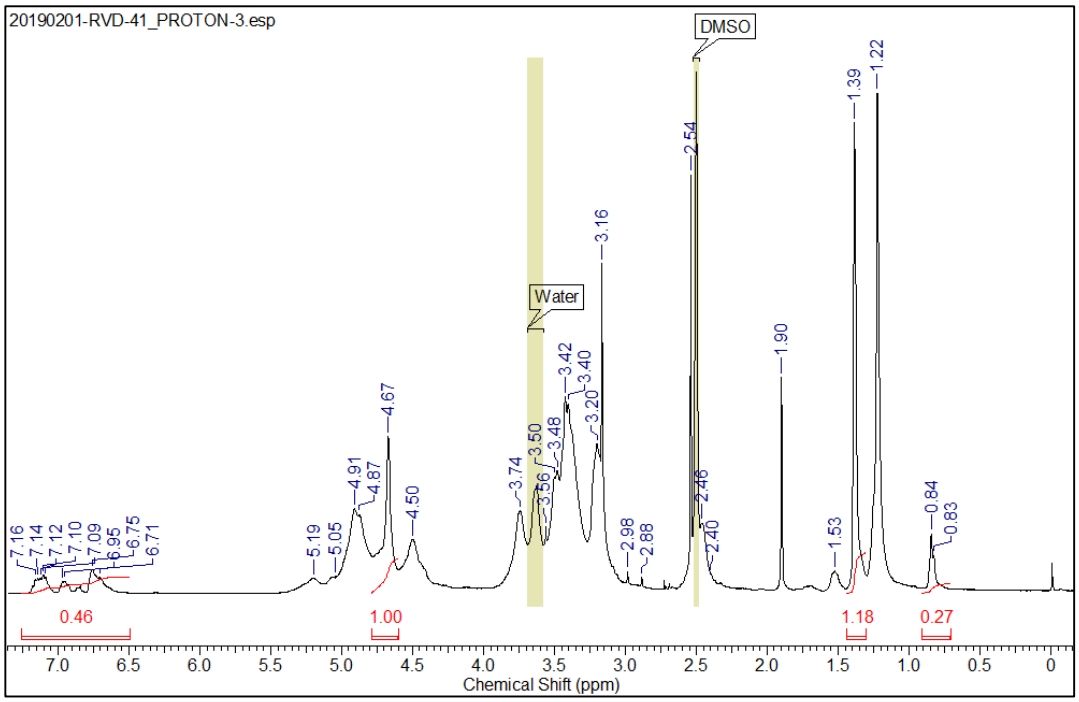

Figure 3.9. ^{1}H NMR of DEX-PDP-TPE-SA

The formation of the dextran polymer was confirmed via ^{1}H proton NMR. Giving the anomeric proton an integration of 1 hydrogen, the degree of substitution for each unit was calculated. The percentage substitution was calculated for each unit and was found to be 1%, 13% and 9% for TPE acid, succinic acid – ester and PDP acid respectively.

To conjugate the drug on the polymer backbone, the polymer was first deprotected using trifloroacetic acid (TFA) to obtain the acid functional handle. The disappearance of the peak corresponding to the *tert*- butyl group (as depicted in the figure (3.10)) in the NMR spectra confirms the de-protection of the succinic acid- ester.

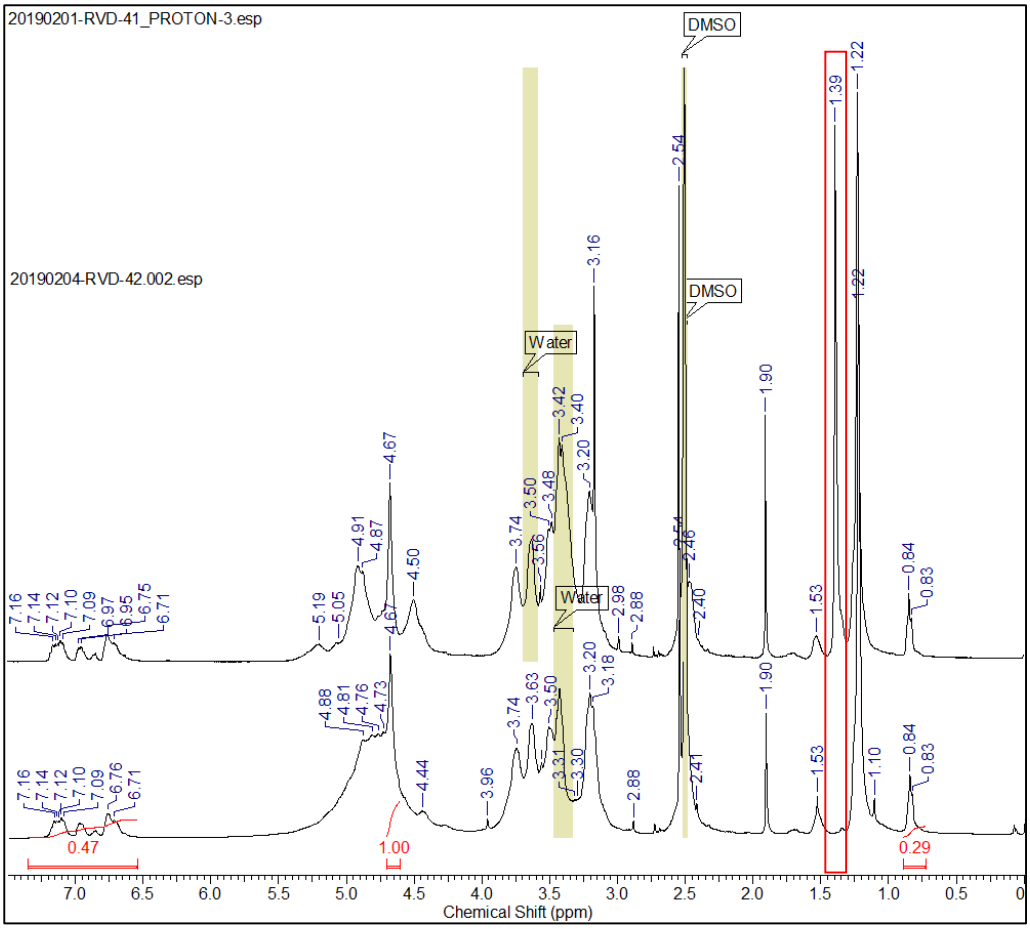

Figure 3.10. ^{1}H NMR of DEX-PDP-TPE-SA (deprotected)

The cisplatin aqua complex was made by $AgNO_3$ treatment of the cisplatin drug along with mili-Q water. AgCl precipitate was formed during this process which was then removed by filtration. Further to acquire a chemical conjugation between the drug and the polymer, the polymer was first dissolved in mili-Q water and treated with 200 µL of NaOH (1mg/mL) solution to obtain a sodium salt of the polymer. Cisplatin aqua complex was then added to this system and stirred in dark for 48 h. A 1:1.1 mole % ratio of acid functionality to cisplatin aqua complex was maintained so as to ensure a 100% conjugation of the drug on the polymer scaffold. After conjugation, the polymer was filtered, lyophilized and stored at 4ºC. Amount of cisplatin stitched to the polymer was calculated using the *Ortho*- phenyldiamine (OPD) assay. OPD binds to the cisplatin stitched onto the polymer backbone to form an OPD – cisplatin complex which shows an absorbance maxima at 706 nm. By monitoring the absorbance of this complex, the DLC and DLE were calculated and found to be 3.2% and 18.9% respectively

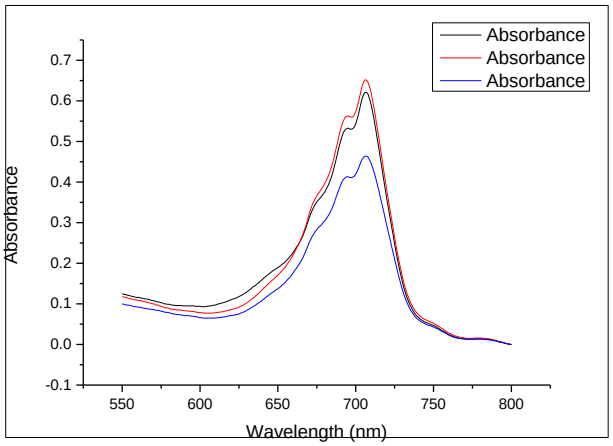

Figure 3.11. Absorption curve of OPD – Cisplatin complex

An IR spectra was recorded for the cisplatin stitched polymer to confirm the chemical conjugation of the drug. A peak at 1650 cm^{-1} corresponding to the Pt-O-C=O stretching frequency was observed along with a peak at 470 cm^{-1} corresponding to the Pt-O alkoxide bond stretching frequiency. It thus confirmed the chemical linkage of the drug onto the polymer backbone.

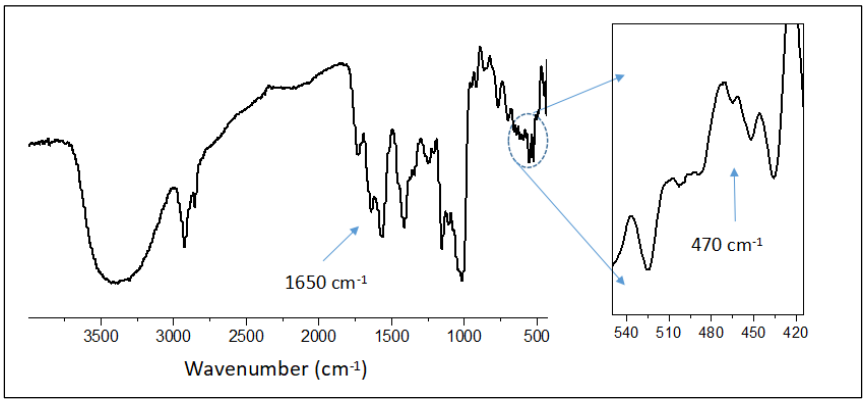

Figure 3.12 IR spectra of the cisplatin stitched DEX-PDP-TPE-SA polymer

3.3 Self-assembly and morphological studies

Both the analogues (cisplatin stitched polymer and the acid counterpart) were subjected to self-assembly via dialysis method through a semipermeable membrane of MWCO = 3500 g/mol to obtain a (5mg / mL) solution of the self-assembled system. The self-assembly was further studied by characterization through techniques like DLS and FESEM to understand the size and morphology of the system. Dynamic Light Scattering (DLS) was used as a tool to obtain the size range for these polymers and it

was observed that the size distribution of the self-assembled system lies between 150 ± 15 nm and 145 ± 15 nm for the polymer alone and Rhodamine –B loaded system respectively. These values correspond to the DLS measurements before cisplatin stitching and are shown in (fig 3.13 a and b). Further, the cisplatin stitched polymer was also self-assembled in the similar fashion to check the consequence of Cisplatin stitching on nano-structure size and morphology. The nano-assemblies showed a size of 170 ± 20 nm and 150 ± 20 nm for cisplatin stitched polymer alone and Rhodamine –B loaded system respectively.

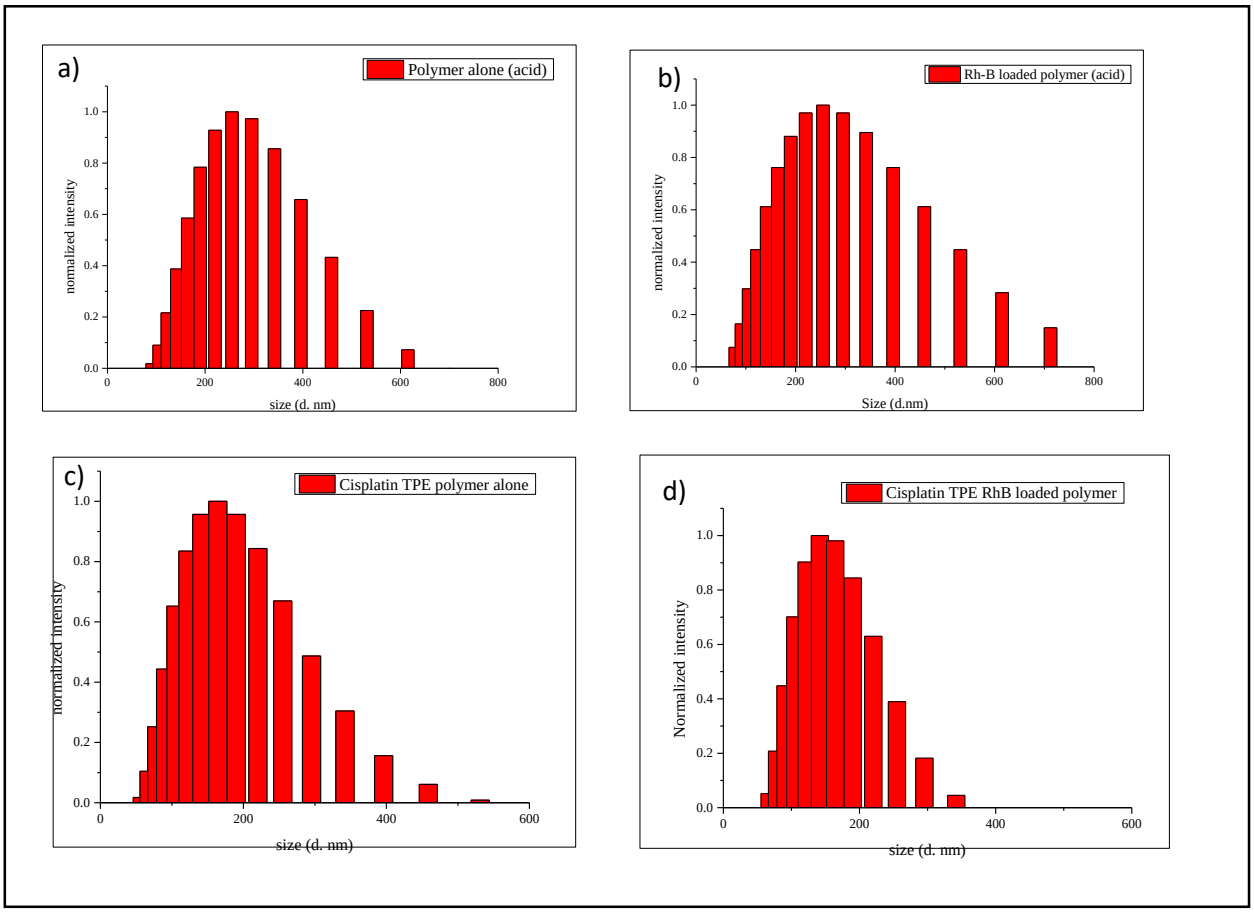

Figure 3.13 a) DLS histogram of DEX-PDP-TPE-SA (top left image), b) DLS histogram of Rhodamine-B loaded DEX-PDP-TPE-SA (top right image), c) DLS histogram of DEX-PDP-TPE-Cisplatin (bottom left image), d) DLS histogram of Rhodamine – B loaded DEX-PDP-TPE-Cisplatin (bottom right image).

The DLC and DLE were calculated and found to be 1.5% and 15% respectively for the DEX-PDP-TPE-SA acid polymer. On cisplatin stitching, the DLC and DLE were found to be 2.0% and 20.3% respectively for the Rhodamine-B loaded polymer after cisplatin stitching. Thus, it can be concluded that Cisplatin stitching does not disturb the size of the polymer. Also an increase in DLC and DLE is observed upon cisplatin stitching of

the polymer which indicates the compact packing of the vesicles aided by cisplatin stitching. Further, the size and morphology of the self-assembeled structures were studied using FESEM. Fig(3.14 (a)) shows the donut shaped structure which confirms the formation of vesicular self-assemblies. The sizes of the nanovesicles were obtained to be around 160 ±30 nm before cisplatin stitching (see figure 3.14 c) and about 130 ± 10nm after cisplatin stitching (see figure 3.14 d) which is consistent with the sizes obtained from the DLS measurements. Also, Rhodamine – B loading and cisplatin stitching of the polymer did not change the morphology of the vesicles (figure 3a and 3b).

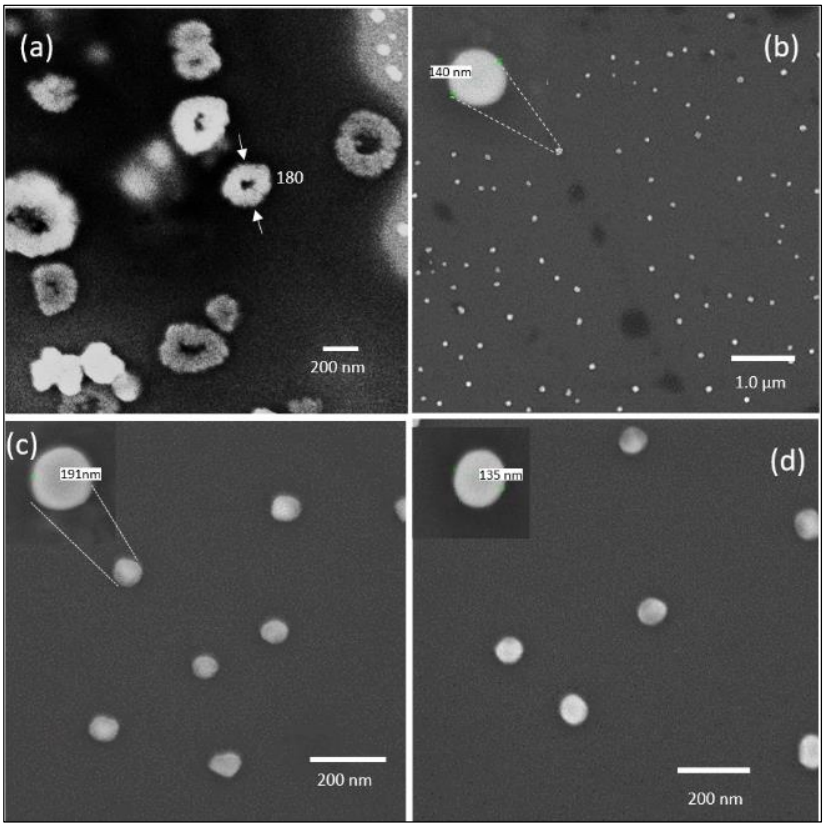

Figure 3.14 a) FESEM image of DEX-PDP-TPE-SA (first row, left image), b) FESEM image of Rhodamine-B loaded DEX-PDP-TPE-SA (first row, right image), c) FESEM image of DEX-PDP-TPE-Cisplatin (second row,left image), d) FESEM image of Rhodamine-B loaded DEX-PDP-TPE-SA-Cisplatin (second row, right image).

3.4 Photophysical properties of the fluorescent derivative

TPE exhibits a unique property of aggregation induced emission and gives an absorption maxima at 313 nm. To study the photophysical properties of the fluorescent polymer, 0.1 OD solution with respect to TPE were made, and was maintained throughout all the studies. TPE and Rhodamine – B were found to make a FRET pair and the same can be seen through the graph in fig (3.15). Upon being excited at 330 nm (λ excitation of TPE) , an emission PL intensity of about 50,000 by TPE- polymer alone system was observed(represented by the black line in graph 1 fig (3.15)). Whereas , after loading this polymer with Rhodamine-B and exciting the system at 330 nm, a complete disappearance of the TPE emission was observed along with the appearance of a new peak at 570 nm corresponding to the emission from Rhodamine – B. This phenomenon is observed because the TPE chromophore transfers its energy to the Rhodamine-B molecules as a result of which there is a complete disappearance of its emission intensity and the dye emission peak can be seen (represented by the red line in graph 1 fig(3.15 (a))). The blue line the graph represents the emission from the Rhodamine-B loaded polymer upon being excited at Rhodamine-B excitation wavelength. From the graph, it is evident that there is an efficient FRET between TPE and Rhodamine-B. Similar studies were performed after cisplatin stitching of the polymer and it gave similar results as we can see in the fig(3.15 (b)). Thus, it can be concluded that Cisplatin stitching doesn't interfere with the FRET between TPE and Rh-B. The designed system can therefore be used as a FRET probe to monitor the cisplatin delivery to the cancer cells.

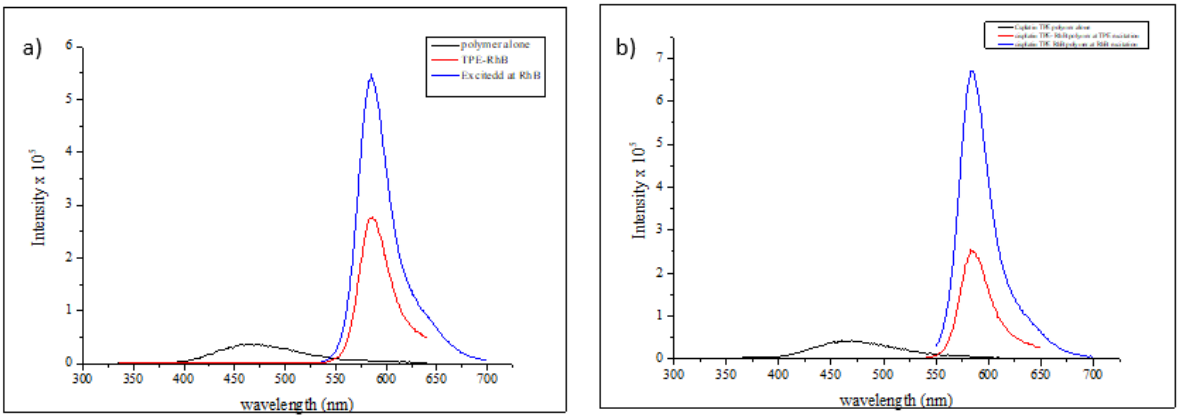

Figure 3.15 a) emission intensity at TPE excitation and FRET between DEX-PDP-TPE-SA and Rh-B loaded DEX-PDP-TPE-SA; b) emission intensity at TPE excitation and FRET between DEX-PDP-TPE-SA-Cisplatin and Rh-B loaded DEX-PDP-TPE-SA-Cisplatin.

Since the emission from the TPE chromophore is based on the phenomena of aggregation induced emission (AIE), fluorescence intensity studies with varying concentrations of DMSO and water were done to study the effect of the change in the solvent environment on the emission of the TPE chromophore incorporated polymer vesicles. It was observed that, maximum PL Intensity was obtained with 100% water as the solvent system. Whereas, with the increase in the percentage of DMSO in the solvent environment, a decrease in the emission from the aggregated TPE molecules is observed (figure (3.16 (a)). By plotting a graph of the PL intensity versus the DMSO concentration in the system, the minimum percentage concentration for obtaining an emission from the aggregated TPE chromophore was determined. Fig(3.16 (b)) shows that the TPE emission from the aggregated state was observed upto 50 % DMSO in water concentration which suggest a break point of self-assembly disruption in the presence of DMSO.

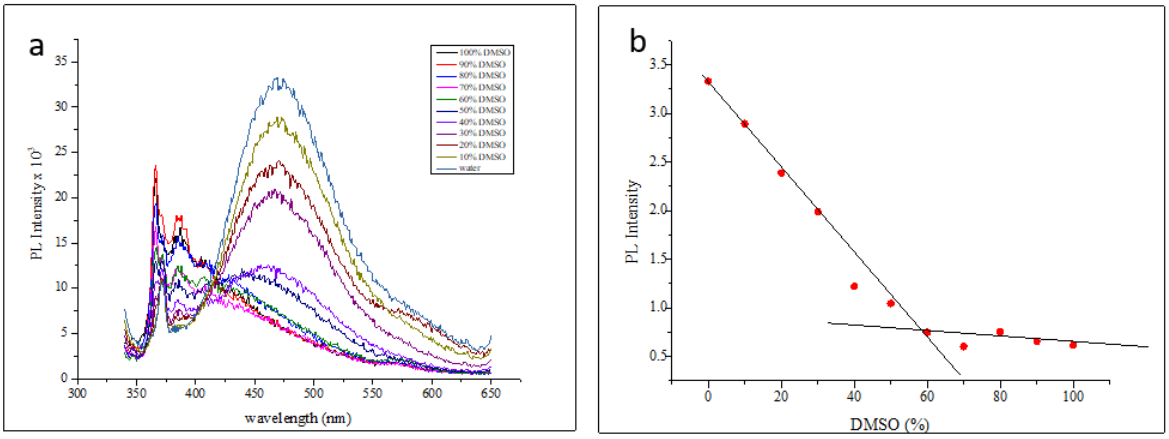

Figure 3.16 a) emission intensity graph of the DEX-PDP-TPE-SA polymer with the change in DMSO concentration; b) Graph depicting change in intensity with varying % DMSO concentration

Figure (3.17) shows the cisplatin stitched polymer and its Rhodamine-B loaded counterpart in dark and under long UV light. The pink colour in the fig(3.17) (a) is because of the rhodamine loading . Both the polymers are non-fluorescent in dark. However,a strong fluorescence can be seen from the vials when kept under the long UV light. The blue colour is due to the emission from the TPE chromophore while the Rhodamine –B loading gives an orange emission.

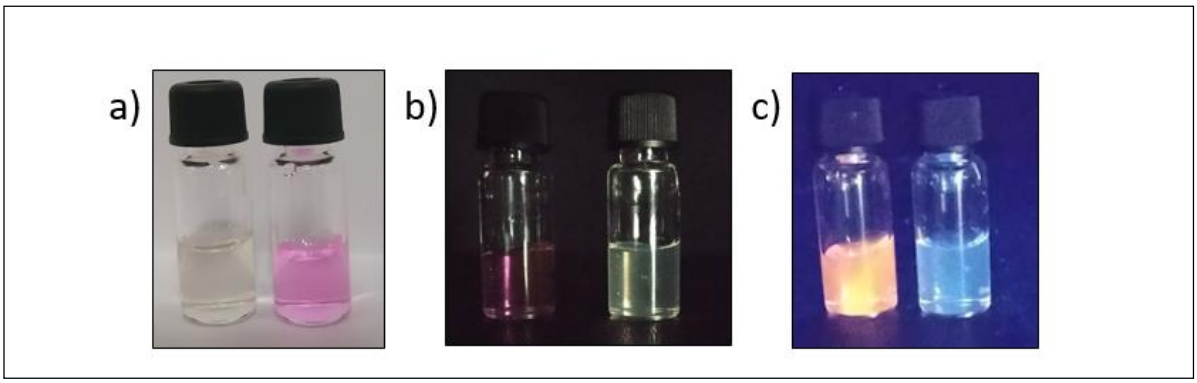

Figure 3.17 a) Cisplatin stitched DEX-PDP-TPE-SA (left vial) and its Rhodamine –B loaded counterpart (right vial) (left image); b)Cisplatin stitched DEX-PDP-TPE-SA (right vial) and its Rhodamine –B loaded counterpart (left vial) in dark (middle image) ; c) Cisplatin stitched DEX-PDP-TPE-SA (right vial) and its Rhodamine –B loaded counterpart (leftt vial) under long UV light (right image).

3.5 Release studies

As the monomers are anchored to the dextran polymer backbone via aliphatic ester bonds, polymer degradation studies were done using esterase enzyme to check the biodegradability and release kinetics of the system. Esterase is known to cleave the aliphatic ester bonds and is present in the lysosomal compartment of the cells. Thus, the nanocarrier would disrupt after being acted upon by the enzyme, once into the cell, resulting in the release of the loaded cargo. To study the time dependent release of the loaded cargo, 3.0 mg of Rhodamine-B loaded polymer was dissolved along with 10 U of esterase to obtain a 1.0 mL solution. This was then transferred to the dialysis bag (MWCO = 3500) and 10 mL PBS pH 7.4 was used as the reservoir. Dialysis was done for 48 h at 37ºC. Similarly, Rhodamine-B loaded polymer was dissolved to obtain a 1 mL solution without the addition of esterase enzyme and was dialysed against 10 mL PBS pH 7.4 for 48 h at 37ºC. This acted as a control experiment to check the stability and release of the cargo in the absence of the enzyme.

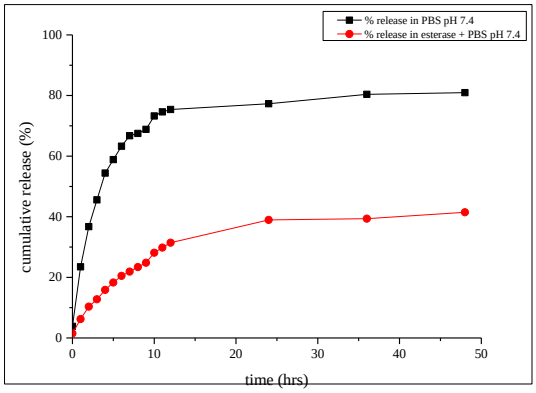

Figure3.18 Release kinetics of Rhodamine-B from the DEX-TPE-PDP-SA polymer

It was observed that about 40% of the loaded cargo was found to leach out of the nanocarriers over a period of 48 h in absence of the esterase enzyme. While, in the presence of the enzyme, about 60 % release can be seen during the first 6h and a total of about 80% release is seen over a period of 48 h. This can be seen in the figure (3.18) showing the release profile of the Rhodamine- B loaded vesicles. This has to be repeated in triplicates to account for the error bar. This would be done in the due period.

3.6 MTT assay

To check the effect of the cisplatin stitched polymer on the cancer cells, MCF-7 breast cancer cells were treated with varying concentrations (0.1µg/mL to 8µg/mL) of cisplatin stitched polymer. MTT or the tertazolium salt undergoes reduction in the viable cells when acted upon by the oxidoreductase enzymes. As a result, MTT gets reduced to form insoluble formazan crystals (purple in colour). These crystals were dissolved in DMSO followed by recording absorbance measurements. Thus a darker purple colour indicates more no. of viable cells. Fig (3.19) shows the cytotoxicity of the DEX-PDP-TPE-Cisplatin and Rh-B loaded DEX-PDP-TPE-Cisplatin polymer. Almost equivalent killing compared to free drug administration can be seen from the plot. Almost 70 % killing was observed after treatment of cells with a concentration of 8µg/mL as shown in figure (3.19). Time dependent uptake studies, MTT assay for polymer alone system and confocal imaging are still under progress.

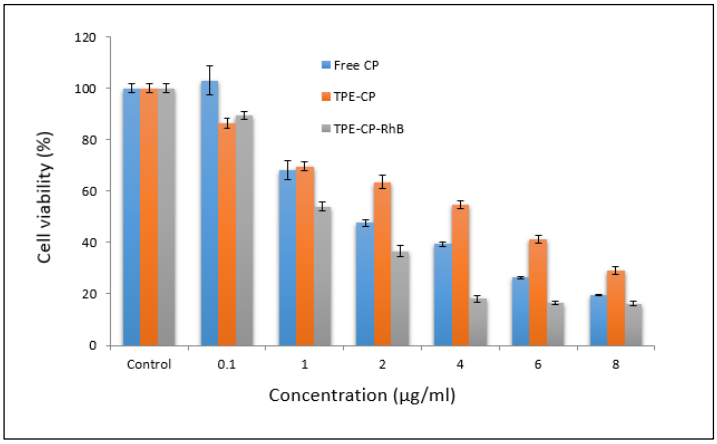

Figure 3.19 A plot showing the cytotoxicity of DEX-PDP-TPE-Cisplatin and Rh-B loaded DEX-PDP-TPE-Cisplatin in MCF-7 breast cancer cell line.

4. Conclusion

Thus, Aggregation Induced Emission (AIE) based fluorescent dextran polymer for cisplatin delivery to the cancer cells was successfully designed and synthesised. Cisplatin drug was chemically conjugated to the polymer backbone and this polymer was further studied by doing self-assembly studies. Photo-physical studies were carried out to study the fluorescent nature of the polymer. The polymer was also loaded with Rhodamine-B and the interaction between the two chromophores was studied. These chromophores make an excellent FRET pair and the FRET between the two chromophores was studied by monitoring the emission intensity of the chromophores. Further, a release kinetics was done to check the biodegradability of the polymer and about 80% release of the loaded cargo was achieved upon degradation by esterase enzyme. An MTT assay was done to see the killing in MCF - 7 Breast cancer cells which showed about 70% killing with a concentration of 8µg/mL.

4.1 Future Perspective

Enzyme triggered release of the cisplatin drug is under study. Bio- imaging using the polymer system and their uptake studies are in progress.

5.References

1. This is taken from www.who.int
2. Iqbal, J., Abbasi, B.A., Ahmad, R. et al. *Appl Microbiol Biotechnol.* **2018** ,*102*, 9449.
3. Rosenblum, D. ; Joshi, N.; Tao, w.; Karp, J.M.; Peer, D. Progress and challenges towards targeted delivery of cancer therapeutics. *Nat. Commun.* **2018**, *9*,1410.
4. Sun, Q.; Sun, X.; Ma, X.; Zhou, Z.; Jin, E.; Zhang, B.; Shen, Y.; Van Kirk, E.A.; Murdoch, W.J.; Lott, J.R.; Lodge, T.P.; Radosz, M.; Zhao, Y. Integration of Nano-assembly Functions for an Effective Delivery Cascade for Cancer Drugs. *Adv. Mater.* **2014**, *26*, 7615-7621.
5. Senapati, S., Mahanta, A. K., Kumar, S. & Maiti, P. Controlled drug delivery vehicles for cancer treatment and their performance. *Sci. Rep* (**2018**),*3*, 7
6. Saha, R. N.; Vasanthakumar, S.; Bende, G.; Snehalatha, M. Nanoparticulate drug delivery systems for cancer chemotherapy*. Mol. Membr. Biol.* **2010**, *27*, 215–231
7. Deshpande, N.U.; Jayakannan, M. Biotin-Tagged Polysaccharide Vesicular Nanocarriers for ReceptorMediated Anticancer Drug Delivery in Cancer Cells : *Biomacromolecules,* **2018**, *19*, 3572−3585.
8. Chauhan, V.P.; Jain, R.K. Strategies for advancing cancer nanomedicines *Nat. Mater.* **2013**, *12(11),* 958- 962.
9. Barenholz, Y. Doxil®—the first FDA-approved nano-drug: lessons learned. *J. Control. Release* **2012**,*160*, 117–134.
10. Su, J., Chen, F., Cryns, V. L. & Messersmith, P. B. Catechol polymers for pHresponsive, targeted drug delivery to cancer cells. *J. Am. Chem. Soc.* **2011** *133*, 11850–11853.
11. Shim, M. S. & Kwon, Y. J. Stimuli-responsive polymers and nanomaterials for gene delivery and imaging applications. *Adv. Drug Deliv. Rev.***2012**, *64*, 1046–1059.
12. Mo, R., Jiang, T. & Gu, Z. Recent progress in multidrug delivery to cancer cells by liposomes. *Nanomedicine* **2014** ,*9*, 1117–1120.
13. Shi, J.; Kantoff, P.W.; Wooster,R.; Farokhzad, O.C. Cancer nanomedicine: progress, challenges and opportunities. *Nat. Rev Cancer.* **2017**, *17* , 20-37.

14. Abdalla, A.M.E.; Xiao, L.; Uallah, M.W. ; Yu, M.; Ouyang, C.; Yang, G. Current Challenges of Cancer Anti- angiogenic Therapy and the Promise of Nanothereputics. *Theranostics*, **2018**, *8*, 533-548.
15. Matsumura, Y. & Maeda, H. A new concept for macromolecular therapeutics in cancer chemotherapy: mechanism of tumoritropic accumulation of proteins and the antitumor agent smancs. *Cancer Res.* **1986** , *46*, 6387–6392 .
16. Peer, D.; Karp, J.M.;Hong, S.P.;Farokhzad, O.C.; Margalit, R.; Langer, R. Nanocarriers as an emerging platform for cancer therapy. *Nat. Nano* **2007** *2*, 751–760.
17. Byrne, J. D.; Betancourt, T.; Brannon-Peppas, L. Active targeting schemes for nanoparticle systems in cancer therapeutics. *Adv. Drug Deliv. Rev*. **2008**, *60*, 1615–1626.
18. Tran, S.; DeGiovanni, P.J.; Piel, B.; Rai, P. Cancer nanomedicine: a review of recent success in drug delivery. *Clin. Transl. Med.* **2017**, *6,* 44.
19. Mizrahy, S.; Peer, D. Polysaccharide as Building Block For Nanotherepeutics. *Chem. Soc. Rev.* **2012**, *41*, 2623−2640.
20. Wen, Y.; Oh, J. K. Recent Strategies to Develop PolysaccharideBased Nanomaterials for Biomedical Applications. *Macromol. Rapid Commun***. 2014**, *35*, 1819−1832.
21. Lemarchand, C.; Gref, R.; Passirani, C.; GArcion, E.; Petri, B.; Muller, R.; Costantini, D.; Couvreur, P. Influence of Polysaccharide Coating on the Interaction of Nanoparticles With Biological Systems. *Biomaterials* **2006**, *27*, 108−118.
22. Bao,Y.; Guegain, E.; Nicolas, V.; Nicolas, J. Fluorecent ppolymer prodrug nanoparticles with Aggregation Induced Emission (AIE) properties from nitro-oxide mediated polymerization. *Chem. Commun*. ,**2017**, *53*, 4489
23. Hong, Y.; Lam, J.W.Y.; Tang, B.Z. aggregation induced emission: phenomenon, mechanism and application. *Chem. Commun*.,**2009**, 4332-4353
24. Pramod, P.S.; Takamura, K.; Chaphekar, S.; Balasubramanian, N.; Jayakannan, M. Dextran vesicular carriers for Dual Encapsulation of Hydrophilic and Hydrophobic Molecules and Delivery into cell. *Biomacromolecules*, **2012**, *13*, 3627-3640

25. Deshpande, N.U.; Jayakannan, M. Cisplatin-Stitched Polysaccharide Vesicles for Synergistic Cancer Therapy of Triple Antagonistic Drugs *Biomacromolecules,* **2017***,18,* 113-126.
26. Long Jr, D.M.; Sanchez, L.; Varco, R.L.; Lillehei, C.W. The use of low molecular weight dextran and serum albumin as plasma expanders in extracorporeal circulation *Surgery*, **1961**, *50*, 12-28.
27. Surnar, B.; Sharma,K.; Jayakannan, M. Core- shell Nanoparticles for prevention of GSH drug detoxification and Cisplatin delivery to breast cancer cells. *Nanoscale*, **2015**,*7,* 17964-17979.